JOURNAL OF VIROLOGY, July 2006, p. 6964–6972 Vol. 80, No. 14
0022-538X/06/$08.00+0 doi:10.1128/JVI.00024-06

Hepatitis C Virus Entry Depends on Clathrin-Mediated Endocytosis

Emmanuelle Blanchard,[1] Sandrine Belouzard,[1] Lucie Goueslain,[1] Takaji Wakita,[2] Jean Dubuisson,[1] Czeslaw Wychowski,[1] and Yves Rouillé[1]*

CNRS-UMR8161, Institut de Biologie de Lille and Institut Pasteur de Lille, Lille, France,[1] and Department of Virology II, National Institute for Infectious Diseases, Tokyo, Japan[2]

Received 4 January 2006/Accepted 3 May 2006

Due to difficulties in cell culture propagation, the mechanisms of hepatitis C virus (HCV) entry are poorly understood. Here, postbinding cellular mechanisms of HCV entry were studied using both retroviral particles pseudotyped with HCV envelope glycoproteins (HCVpp) and the HCV clone JFH-1 propagated in cell culture (HCVcc). HCVpp entry was measured by quantitative real-time PCR after 3 h of contact with target cells, and HCVcc infection was quantified by immunoblot analysis and immunofluorescence detection of HCV proteins expressed in infected cells. The functional role of clathrin-mediated endocytosis in HCV entry was assessed by small interfering RNA-mediated clathrin heavy chain depletion and with chlorpromazine, an inhibitor of clathrin-coated pit formation at the plasma membrane. In both conditions, HCVpp entry and HCVcc infection were inhibited. HCVcc infection was also inhibited by pretreating target cells with bafilomycin A1 or chloroquine, two drugs known to interfere with endosome acidification. These data indicate that HCV enters target cells by clathrin-mediated endocytosis, followed by a fusion step from within an acidic endosomal compartment.

Hepatitis C virus (HCV) infects about 170 million people around the world. Despite the importance of HCV as a human pathogen, little is known about its cell biology. The virus was identified and cloned more than 15 years ago (7), but the lack of a robust system allowing for the production of HCV in cell culture has hampered for many years functional studies on HCV infection.

In recent years, two major advances have made it possible to investigate HCV entry. A first advance has been the production of infectious retroviral particles pseudotyped with HCV envelope glycoproteins (3, 14, 24). Using this system of HCV pseudoparticles (HCVpp), observations on receptor usage and the facilitating role of high-density lipoprotein during entry were reported (3, 24, 55). A second major advance has been the recent development of a cell culture model for HCV (30, 56, 59). This system allows for the production of virus that can be efficiently propagated in cell culture (HCVcc). Therefore, the cell entry of HCV can now be investigated in the context of an infectious cycle.

HCV belongs to the *Hepacivirus* genus in the *Flaviviridae* family, which also includes the *Flavivirus* and *Pestivirus* genera (31). The HCV genome encodes three structural proteins, capsid protein C and envelope glycoproteins E1 and E2, which are associated in the form of a heterodimer (13). Several cellular proteins were reported to interact in vitro with isolated E2. These putative receptors include the tetraspanin CD81 (42), the scavenger receptor class B type I (SR-BI) (50), the lectins L-SIGN and DC-SIGN (18, 32), the asialoglycoprotein receptor (49), and heparan-sulfate proteoglycans (2). The low-density lipoprotein receptor was also proposed as a candidate receptor (1). The importance of CD81 and SR-BI in HCV entry was confirmed with HCVpp (3, 4, 24) as well as with HCVcc for CD81 (30, 56). Beyond receptor binding, virtually nothing is known about molecular and cellular mechanisms used by HCV during cell entry.

According to postbinding mechanisms of entry, enveloped viruses fall into two main types. Some viruses deliver their genome to the cytosol of target cells by fusing their envelope with the plasma membrane, while other ones enter by endocytosis. For many enveloped viruses that enter cells by endocytosis, an activation step occurs in endosomes which leads to the fusion of the viral envelope with the membrane of the endosome and the delivery of the viral genome into the cytosol. The acidic pH of endosomes is thought to play an essential role in triggering this fusion event, which is catalyzed by a viral envelope glycoprotein. Therefore, the pH sensitivity is often considered a good indication of entry by endocytosis. The best documented mode of endocytosis is the clathrin-mediated pathway. However, recent studies have revealed a surprising variety of endocytic routes (10, 39, 51).

Previous reports have indicated a pH dependency for HCVpp entry (4, 24), suggesting that HCV would enter cells by endocytosis. However, the functional importance of endocytosis in HCV infection has not been directly tested so far, and the endocytic pathway used by the virus has not been identified. In this paper, we report on postbinding cellular mechanisms of HCV entry. Using both a newly developed HCVpp entry assay and the JFH1-based HCVcc model, we confirmed the pH sensitivity of HCV entry and established the functional importance of clathrin-mediated endocytosis in HCV entry.

MATERIALS AND METHODS

Chemicals. Dulbecco's modified Eagle's medium (DMEM), phosphate-buffered saline (PBS), OptiMEM, HEPES, and goat and fetal calf sera (FCS) were purchased from Invitrogen. Hoechst dye 33342 was from Molecular Probes. Chlorpromazine was from Alexis. Bafilomycin-A1 and Mowiol 3-88 were from

* Corresponding author. Mailing address: Équipe Hépatite C, CNRS-UMR8161, Institut de Biologie de Lille, 1 rue du Professeur Calmette, BP447, 59021 Lille cedex, France. Phone: (33) 3 20 87 10 27. Fax: (33) 3 20 87 12 01. E-mail: yves.rouille@ibl.fr.

Calbiochem. ExGen500 was purchased from Euromedex. All other chemicals were from Sigma.

Antibodies. Rat monoclonal antibody (MAb) 3/11 (17) and mouse MAb A4 (15) were produced in vitro by using a MiniPerm apparatus (Heraeus) as recommended by the manufacturer. Anti-NS3 (486D39) MAb was kindly provided by J. F. Delagneau (Bio-Rad, France). Mouse anti-E2 MAb AP33 (9) was kindly provided by A. H. Patel (Institute of Virology, Glasgow, United Kingdom). Mouse anti-clathrin heavy chain (CHC) MAb was purchased from BD Biosciences. Goat anti-actin polyclonal antibody and mouse anti-simian virus 40 (SV40) T-antigen MAb (Pab101 [sc-147]) were from Santa Cruz. Anti-green fluorescent protein (GFP) MAb was from Roche. Alexa594-conjugated or Alexa555-conjugated goat anti-mouse secondary antibody was from Molecular Probes.

Cell culture. 293T human embryo kidney cells (HEK 293T), PLC/PRF/5 human hepatoma cells (ATCC CRL-8024), and Huh-7 human hepatoma cells were grown in Dulbecco's modified essential medium supplemented with glutamax and 10% fetal bovine serum.

Production of HCVpp. Pseudotyped particles were produced as described previously (3). Plasmids were kindly provided by D. Lavillette, B. Bartosch, and F.-L. Cosset (INSERM U412, Lyon, France). Briefly, 293T cells were cotransfected with a murine leukemia virus (MLV)-based transfer vector encoding luciferase (37), a murine leukemia virus Gag-Pol packaging construct, and an envelope glycoprotein-expressing vector, phCMV-E1E2 (3), using Exgen 500 as recommended by the manufacturer. The phCMV-G, phCMV-RD114, phCMV-A, and phCMV-HA expression vectors encode the vesicular stomatitis virus G protein (VSV-G), the feline endogenous virus RD114 glycoprotein, the MLV 10A1 envelope glycoprotein (A-MLV), and the fowl plague virus H7 hemagglutinin (HA), respectively (48). The phCMV-NA expression vector for influenza virus neuraminidase (NA) was a kind gift from F.-L. Cosset. Pseudotyped particles harboring VSV-G, RD114, A-MLV, or hemagglutinin (HA) and NA envelope glycoproteins on murine leukemia virus cores (VSV-Gpp, RD114pp, A-MLVpp, and HA/NApp, respectively) were used as controls. Supernatants containing the pseudotyped particles were harvested 48 h after transfection, filtered through 0.45-μm-pore-sized membranes, and incubated with 300 U/ml DNase I (Roche) for 30 min at 37°C to remove excess plasmid DNA. Pseudotyped particle stocks were kept at 4°C and used within 1 week after production. The luciferase-based HCVpp infection assay was as previously described (37).

PCR-based entry assay. Confluent cell monolayers grown in 12-well plates were infected with 600 μl of DNase-treated pseudoparticles in DMEM supplemented with 10% FCS and 20 mM HEPES. The multiplicity of infection was about 1 (range, 0.5 to 1.5). The infection was enhanced by spinoculation, as previously reported for human immunodeficiency virus (36). Plates were enclosed in plastic bags and centrifuged at 1,200 × *g* for 2 h at 37°C and then incubated for 1 h in a 5% CO_2 incubator at 37°C. After 3 h of contact, the cells were washed three times with PBS. Total DNA was extracted using the Wizard SV Genomic DNA Purification System (Promega) according to the manufacturer's instructions. Each sample of DNA was purified from two pooled wells and was dissolved into 200 μl of DNase-free water.

Quantification of early reverse-transcribed viral DNA was performed by quantitative PCR assay. Primers were designed in the U3 region of the long terminal repeat (LTR) of MLV with the help of the Primer3 software (45). The sequences of the forward and reverse U3 primers were 5′-CCATCAGATGTTTCCAGGC T-3′ and 5′-GCGACTCAGTCTATCGGAGG-3′, respectively. DNA was amplified in glass capillaries using a LightCycler instrument (Roche Diagnostics, Meylan, France). The PCR mix contained 4 μl of sample DNA and 16 μl of FastSTART DNA Master SYBR Green I (Roche Diagnostics), 4 mM $MgCl_2$, and 0.5 μM of each primer. The PCR amplification was performed for 40 cycles of 15 s at 95°C, 5 s at 60°C, and 7 s at 72°C. The specificity of the amplicon was determined by using melting curve analysis, which displayed only one peak in agreement with a specific amplicon.

The standard curves for quantification of the U3 LTR region of MLV were constructed with 10-fold serial dilutions ranging from 10^5 to 100 copies of phCMV-Luc plasmid. The standard curve was also used to assess PCR efficiency by examining its slope, which was consistently between −3.45 and −3.3 for each experiment. Individual samples were evaluated in duplicate. Absolute quantification of the viral load was evaluated by using the albumin gene as an internal control gene, as described previously (19). The conditions used to amplify the albumin gene were identical to those used for the U3 LTR region. The infection was scored as the ratio of U3 LTR DNA mean copy number over albumin DNA mean copy number. Background values obtained from parallel infections with pseudoparticles containing no envelope protein were subtracted. Data are presented as the percentage of infection relative to control conditions. Using this assay, HCVpp preparations usually yielded titers between 10^5 and 10^6 infectious units/ml on PLC/PRF/5 cells.

Production of HCVcc. To generate genomic HCV RNA, the plasmid pJFH1 (56) was linearized at the 3′ end of the HCV cDNA by XbaI digestion. Following treatment with mung bean nuclease, the linearized DNA was then used as a template for in vitro transcription with the MEGAscript kit from Ambion. In vitro-transcribed RNA was delivered to Huh-7 cells by electroporation as described previously (25). Viral stocks were obtained by harvesting cell culture supernatants at 1 week posttransfection. Secondary viral stocks were obtained by additional amplifications on naïve Huh-7 cells. Infectious titers of viral stocks were estimated between 10^5 and 10^6 infectious units per ml, based on immunofluorescent detection of infected foci following infection of Huh7 cells with serial dilutions of viral stocks.

Other viruses. The recombinant Sindbis virus expressing HCV envelope protein E1 was previously described (16). Stocks of SV40 virus were previously described (58). The recombinant Sendai virus (SeV) expressing a green fluorescent protein (GFP) was previously described (28). A purified stock of recombinant SeV was kindly provided by Laurent Roux, University of Geneva.

HCVcc infection. For HCVcc infection assays, Huh-7 cells grown in 24-well plates were infected for 2 h at 37°C with HCVcc or control viruses. Each HCVcc stock was concentrated between 5 and 10 times by ultrafiltration using Vivaspin cartridges (molecular weight cutoff, 300,000) in order to get 20 to 40% infected cells. For experiments using small interfering RNA (siRNA), equal numbers of CHC siRNA-treated cells and control siRNA-treated cells were infected. For experiments using chlorpromazine and inhibitors of endosomal acidification, cells were preincubated with inhibitors for 30 min before infection, and the drugs were added to the infection and culture media up to the end of the experiment. In some control experiments, drugs were added at 2 h postinfection (hpi). Infections were scored by immunoblot analysis or by indirect immunofluorescence microscopy at 30 hpi (HCVcc and SV40), 16 hpi (SeV), or 5 hpi (Sindbis virus).

RNA interference. Subconfluent cultures of PLC/PRF/5 or Huh-7 cells in 6-well plates were transfected twice with 80 pmol of synthetic double-stranded siRNA (Dharmacon) complexed with 4 μl of oligofectamine (Invitrogen) in a total volume of 1 ml of OptiMEM for 6 h. The interval between both siRNA transfections was 48 h. Cells were trypsinized 24 h after the second siRNA transfection and plated in 12-well plates for the HCVpp entry assay, or they were plated in 24-well plates for infection with HCVcc and infected 24 h after trypsinization. Just before infection, extra wells of cells treated with each siRNA were counted to ensure that equal numbers of cells were infected. Relative CHC levels were analyzed by immunoblotting equal amounts of cell lysates. The films were scanned and quantified with the Image J software. The CHC target sequence was UAAUCCAAUUCGAAGACCAAU (34). The control siRNA was originally designed to knock down the green fluorescent protein; its target sequence is GCUGACCCUGAAGUUCAUC.

Indirect immunofluorescence microscopy. Infected cells were processed for immunofluorescent detection of viral proteins as previously described (44). Nuclei were stained by a 1-min incubation in PBS containing 1 μg/ml Hoechst dye 33342. Coverslips were mounted on glass slides using Mowiol and observed with a Zeiss Axiophot equipped with a ×40 magnification, 1.3 numerical aperture oil immersion lens. Fluorescent signals were collected with a Princeton cooled charged device using specific fluorescence excitation and emission filters. Images were processed using Adobe Photoshop software. For quantification, images of 10 randomly picked areas of each coverslip were recorded. Cells labeled with anti-E2 MAb AP33 were counted as infected cells. The total number of cells was obtained from Hoechst-labeled nuclei. The infections were scored as the ratio of infected cells to total cells.

Immunoblotting. Cells were lysed in 50 mM Tris-Cl buffer, pH 7.5, containing 100 mM NaCl, 1 mM EDTA, 1% Triton X-100, 0.1% sodium dodecyl sulfate (SDS), and protease inhibitors, for 30 min on ice. Cells were collected, and the nuclei were pelleted. Protein concentration in the postnuclear supernatants was determined by the bicinchoninic acid method as recommended by the manufacturer (Sigma), using bovine serum albumin as the standard. Five micrograms of total protein was separated by SDS-polyacrylamide gel electrophoresis and transferred to nitrocellulose membranes (Hybond-ECL; Amersham) by using a Trans-Blot apparatus (Bio-Rad). The proteins of interest were revealed with specific primary antibodies followed by donkey anti-goat immunoglobulin G (IgG), goat anti-mouse IgG, or anti-rat IgG conjugated to peroxidase (Jackson Immunoresearch) as well as enhanced chemiluminescence detection (Amersham) as recommended by the manufacturer.

RESULTS

Real-time PCR-based HCVpp entry assay. In order to study HCVpp entry, we first tried to use a luciferase-based assay (37). However, our attempts were quite ineffective, due to drug toxicity and differences in cell proliferation under various experimental conditions, over the 2-day culture period that is necessary for luciferase expression. To overcome these difficulties, we set up a new assay for HCVpp entry, derived from the method originally designed by Mothes et al. for studying retrovirus entry (33). It is based on the quantification by PCR of the cDNA synthesized in target cells during HCVpp entry. In order to quantify early events during HCVpp entry, we designed primers in the U3 region of the LTR, which is the first part of the viral genome to be retrotranscribed during the entry of a retroviral particle (21).

During the development of this assay, we observed that HCVpp infection yielded signals about three times higher in PLC/PRF/5 cells than in Huh-7 cells. This effect was observed with the PCR-based assay as well as with the luciferase-based assay (data not shown). Therefore, most of the experiments were carried out in PLC/PRF/5 cells.

Since HCVpp infection is sensitive to agents that neutralize the pH of endosomes (4, 24), we tested whether we could detect this pH sensitivity with the PCR-based assay in order to confirm that it indeed reflects this entry pathway. The importance of endosome acidification was studied with bafilomycin A1, which is a specific inhibitor of endosomal proton-ATP pumps. PLC/PRF/5 cells were preincubated for 30 min with various concentrations of bafilomycin A1 and infected in the presence of the inhibitor. Results (Fig. 1A) show that the amounts of retroviral DNA recovered from infected cells dramatically decreased for HCVpp and VSV-Gpp in a dose-dependent manner. In contrast, the synthesis of A-MLVpp-derived retroviral DNA was not affected by 20 or 50 nM bafilomycin A1, and it was reduced at 100 nM. Although significant, this reduction was much smaller than that observed for HCVpp and VSV-Gpp at the same concentration. A similar partial inhibition of A-MLVpp infection with 100 nM bafilomycin A1 was previously reported (4). Similar inhibitions of HCVpp and VSV-Gpp infection were observed with Huh-7 cells (data not shown). Inhibition of HCVpp and VSV-Gpp entry, but not of A-MLVpp entry, was also observed in the presence of chloroquine or NH_4Cl in PLC/PRF/5 cells as well as in Huh-7 cells (data not shown). The results obtained with these different inhibitors of endosomal acidification confirmed that the PCR-based entry assay recapitulates HCVpp entry up to the fusion step.

We next examined whether the levels of retroviral DNA synthesis after 3 h of contact predicted the levels of luciferase expression 3 days later. PLC/PRF/5 cells were infected with different dilutions of an HCVpp stock, and they were then either immediately extracted to purify and quantify retroviral DNA or cultured for 3 days and assayed for luciferase activity. Each assay displayed dose dependency, and interassay comparisons revealed a clear correlation between the level of MLV DNA synthesis and the subsequent level of luciferase expression (Fig. 1B). These results indicate that the levels of DNA synthesis at 3 h accurately quantitate the levels of HCVpp entry.

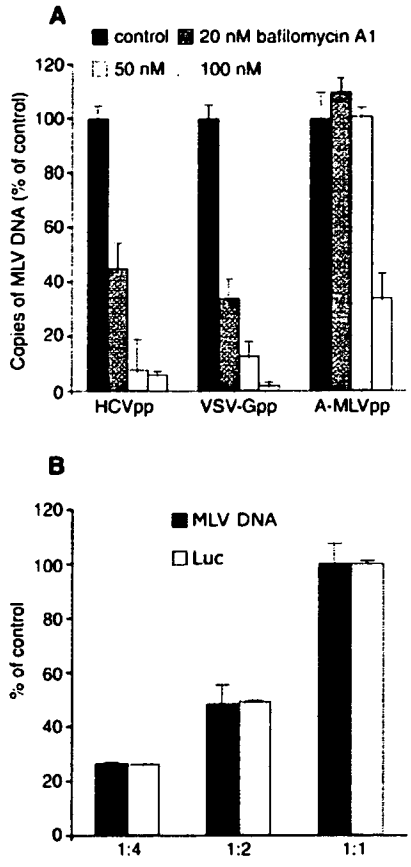

FIG. 1. PCR-based HCVpp entry assay. (A) PLC/PRF/5 cells were pretreated for 30 min with 20, 50, or 100 nM bafilomycin A1 or left untreated. The cells were then infected with HCVpp, VSV-Gpp, or A-MLVpp in the presence of the drug. After 2 h of spinoculation and an additional hour of incubation, total DNA was purified and retroviral DNA was quantified by real-time PCR. Mean values for the controls with no drug were 1.2 equivalent genomes per cell (EG/cell) for HCVpp, 1.5 EG/cell for VSV-Gpp, and 1.3 EG/cell for A-MLVpp infections. The background value obtained from cells infected with pseudotyped particles produced in the absence of envelope proteins corresponded to 0.03 EG/cell. Results were expressed as the percentage of entry in control cells treated with no drug. (B) PLC/PRF/5 cells were infected by spinoculation with different dilutions of the same HCVpp stock. Cells were either immediately lysed to extract DNA or cultured for 3 days to allow for luciferase expression. Retroviral DNA was quantified by real-time PCR (MLV DNA), and infection was quantified by luciferase assay (Luc). Mean values for the undiluted HCVpp infection were 1.3 EG/cell and 6.5×10^6 relative light units (RLU), and the background values obtained from cells infected with pseudotyped particles produced in the absence of envelope proteins corresponded to 0.018 EG/cell and 3.0×10^2 RLU. Results were expressed as the percentage of entry in cells infected with undiluted HCVpp stock (1:1).

HCVpp entry is clathrin dependent. The pH dependency of HCVpp entry implies that HCVpp fusion does not occur at the plasma membrane but from within an intracellular acidic compartment, most probably an endosome. To assess the role of clathrin-mediated endocytosis in HCVpp entry, we first examined the inhibitory effect of chlorpromazine. Chlorpromazine causes clathrin lattice to assemble on endosomal membranes and at the same time prevents the assembly of coated pits at

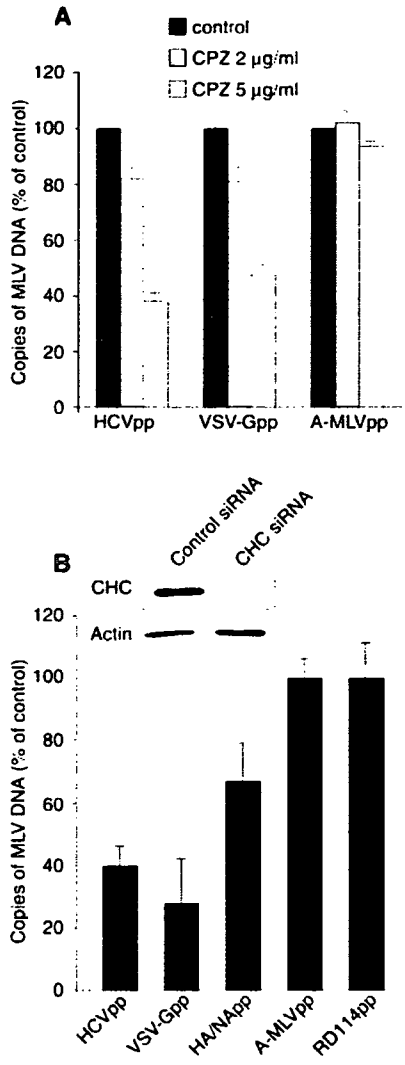

FIG. 2. Clathrin-mediated entry of HCVpp. (A) PLC/PRF/5 cells were pretreated for 30 min with 2 or 5 μg/ml chlorpromazine (CPZ) or were left untreated. The cells were then infected with HCVpp, VSV-Gpp, or A-MLVpp by spinoculation in the presence of the drug. (B) PLC/PRF/5 cells were transfected twice with CHC siRNA or control siRNA, as explained in Materials and Methods. Two days after the second siRNA transfection, cells were spinoculated with HCVpp, VSV-Gpp, HA/NApp, RD114pp, or A-MLVpp. The cellular content of retroviral DNA was quantified by real-time PCR as a measure of entry and is expressed as a percentage of entry in untreated control cells (A) or in cells treated with control siRNA (B). The inset in panel B shows an immunoblot of the relative CHC and actin contents in siRNA-treated cells.

the plasma membrane (57). Chlorpromazine inhibited the entry of HCVpp in PLC/PRF/5 cells in a dose-dependent manner but had minimal effect on A-MLVpp (Fig. 2A). As expected for a clathrin-dependent virus (53), chlorpromazine also inhibited VSV-Gpp entry (Fig. 2A). At 5 μg/ml chlorpromazine, HCVpp entry was inhibited by about 60% and VSV-Gpp entry by about 50%. The use of higher chlorpromazine concentrations resulted in cell detachment during spinoculation of Huh-7 or PLC/PRF/5 cells. This toxicity precluded the use of 10 μg/ml chlorpromazine, a concentration that strongly inhibited bovine viral diarrhea virus infection in MDBK cells (29).

To further confirm that HCVpp entry requires an active pathway of clathrin-mediated endocytosis, we also knocked down the clathrin heavy chain (CHC) using siRNA technology. Following two successive transfections of siRNA, CHC levels were down-regulated to about 20% of controls or less (Fig. 2B). PLC/PRF/5 cells treated with CHC or control siRNA were infected with HCVpp, and entry was quantified by quantitative PCR. For comparison, the entry of retroviral particles pseudotyped with envelope glycoproteins of VSV (VSV-Gpp) or influenza virus (HA/NApp), two viruses known to enter by clathrin-mediated endocytosis, were also quantified. We also monitored the entry of retroviral particles pseudotyped with envelope glycoproteins of two retroviruses known to enter by a nonendocytic route (A-MLVpp and RD114pp). VSV-Gpp entry was strongly inhibited in CHC siRNA-treated cells (Fig. 2B). Similar levels of inhibition were achieved for HCVpp, whereas HA/NApp entry was significantly less inhibited than that of HCVpp and VSV-Gpp, in keeping with the documented dual-entry pathway of influenza virus by both clathrin-mediated and clathrin-independent endocytosis (46, 52). In contrast, the entry of RD114pp or A-MLVpp was not affected by CHC depletion (Fig. 2B), as expected for particles coated with envelope glycoproteins of pH-independent retroviruses. Similar results were obtained with Huh-7 cells (data not shown).

The inhibition of HCVpp entry by chlorpromazine or by CHC depletion strongly suggests that HCVpp enters PLC/PRF/5 cells by clathrin-mediated endocytosis.

HCVcc infection is clathrin dependent. Recently, it has become possible to generate infectious HCV particles in cell culture (HCVcc), allowing the study of HCV entry with infectious viral particles. Preliminary experiments indicated that HCVcc does not infect PLC/PRF/5 cells, in contrast to HCVpp (C. Wychowski, unpublished observation). The reason for this difference is not yet understood, but it may involve a postentry restriction in PLC/PRF/5 cells. Therefore, we used Huh-7 cells to test whether the infection by HCVcc is dependent on clathrin-mediated endocytosis. Huh-7 cells were transfected twice with CHC or control siRNA, infected with HCVcc for 2 h at 37°C, and cultured for 30 h to allow for expression of viral proteins. The cells were then lysed and analyzed by immunoblotting or fixed and processed for immunofluorescence. As shown in Fig. 3A, the expression levels of E2 and NS3 were significantly lower at 30 hpi in CHC siRNA-treated cells than in cells treated with control siRNA or untreated cells. Similar results were obtained at 48 hpi (data not shown).

In comparison, the infection of siRNA-treated Huh-7 cells with Sindbis virus was also monitored. Sindbis virus enters cells by clathrin-mediated endocytosis (6). In order to facilitate the detection of Sindbis virus infection, we used a recombinant Sindbis virus driving the expression of HCV envelope protein E1 in infected cells (16). The infection was detected by immunoblotting cell lysates with anti-E1 (HCV) MAb A4. Note that in these experiments E1 is a transgene that is used as a marker and does not play any role in recombinant Sindbis virus entry. As expected, CHC depletion also had an inhibitory effect on Sindbis virus infection (Fig. 3A).

As a control, we infected siRNA-treated cells with SV40,

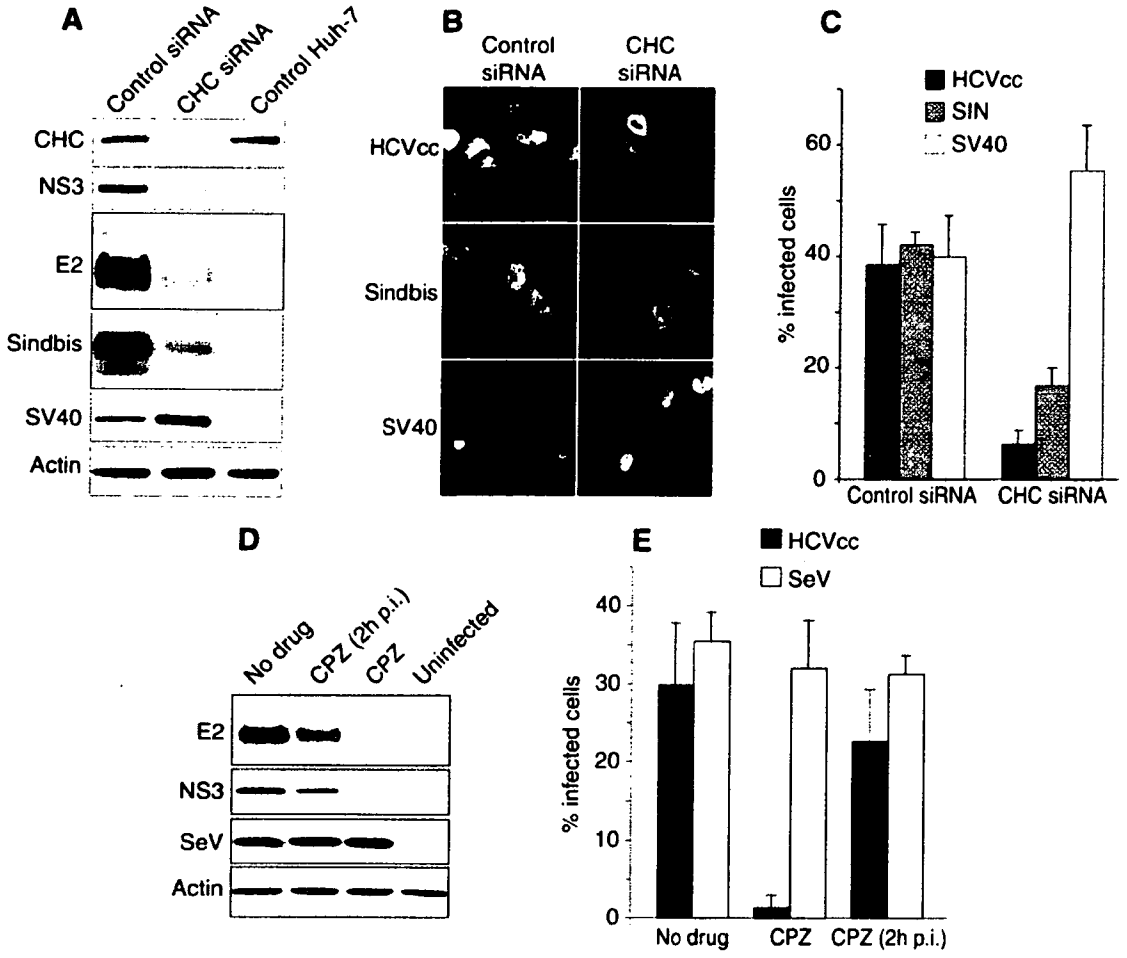

FIG. 3. Clathrin-mediated entry of HCVcc. (A to C) Huh-7 cells were treated with CHC or control siRNA and then infected with HCVcc, a recombinant Sindbis virus expressing HCV E1, or SV40. (A) Cells were lysed at 5 hpi (Sindbis) or 30 hpi (HCVcc and SV40), and the cell lysates were analyzed by immunoblotting with antibodies to E2, NS3 (HCVcc), E1 (Sindbis), T-antigen (SV40), CHC, and actin. (B) Cells were fixed and processed for immunofluorescent detection of E2 (HCVcc), E1 (Sindbis), or T antigen (SV40). (B) For each virus, the fields presented contain similar numbers of CHC or control siRNA-treated cells. (C) Percentage of infected cells in CHC and control siRNA-treated cells. (D and E) Huh-7 cells were pretreated for 30 min and then infected for 2 h with HCVcc in the presence or the absence of chlorpromazine (CPZ; 5 μg/ml). Cells infected in the absence of drug were cultured with no drug, or chlorpromazine was added 2 hpi (CPZ 2hpi). Infection was analyzed (D) by immunoblotting with antibodies to E2, NS3, GFP (SeV), and actin or (E) by immunofluorescent detection of infected cells using an anti-E2 MAb (HCVcc) or by GFP fluorescence (SeV). Results are presented as percentages of infected cells.

which enters by clathrin-independent endocytosis in Huh-7 cells (12). Cells were lysed at 30 hpi, and the levels of T antigen were visualized by immunoblotting. In contrast to HCV and Sindbis virus, SV40 infection was not inhibited in CHC-depleted cells. Instead, we consistently observed in cells treated with CHC siRNA higher levels of T-antigen expression than in cells treated with control siRNA (Fig. 3A). Similar results were obtained with other unrelated control siRNAs (data not shown), thus excluding an inhibitory effect of the control siRNA on SV40 infection or T-antigen expression. This apparent up-regulation of SV40 infection upon CHC depletion was not further investigated in this study.

To verify that the lower levels of HCV proteins observed by immunoblotting resulted from an inhibition of the infection and not from a reduced expression of HCV proteins, infected cells were analyzed by immunofluorescence microscopy. The expression levels of HCV, Sindbis virus, or SV40 proteins in individual cells appeared similar in CHC siRNA-treated cells and in controls (Fig. 3B and data not shown). The number of cells infected by HCVcc was reduced in CHC siRNA-treated cells by about 80% (Fig. 3C). Similar results were obtained when HCVcc infection was scored with an anti-C MAb (data not shown). The number of Sindbis virus-infected cells was also reduced in CHC siRNA-treated cells (by 60%), whereas SV40-infected cells were present in increased numbers (Fig. 3C). These data confirmed the inhibitory role of CHC depletion on HCVcc infection.

The role of clathrin-mediated endocytosis in HCV infection was further confirmed with chlorpromazine. When Huh-7 cells were pretreated with chlorpromazine for 30 min and then infected with HCVcc, the expression levels of E2 and NS3 were dramatically reduced (Fig. 3D) and the number of infected

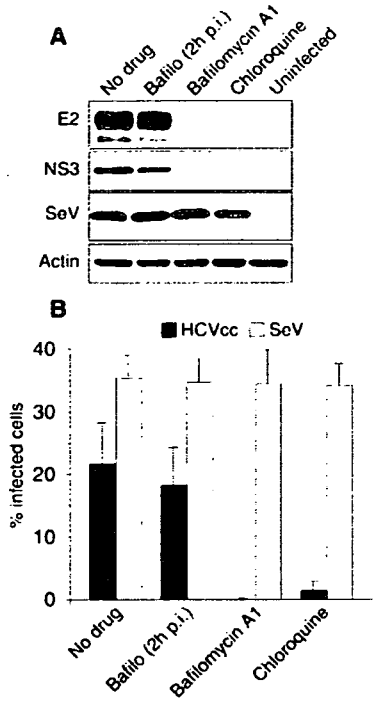

FIG. 4. pH dependency of HCVcc infection. Huh-7 cells were pretreated for 30 min and then infected with HCVcc or SeV in the presence of 50 nM bafilomycin A1 or 20 μM chloroquine or in the absence of any inhibitor of endosomal acidification. Cells infected in the absence of drug were cultured with no drug, or bafilomycin A1 was added 2 hpi (Bafilo 2hpi). HCVcc infection was analyzed (A) by immunoblotting with antibodies to E2, NS3, GFP (SeV) and actin or (B) by immunofluorescent detection of infected cells using an anti-E2 MAb (HCVcc) or by GFP fluorescence (SeV). Results are presented as percentages of infected cells.

cells was very low (Fig. 3E). In contrast, when Huh-7 cells were infected in the absence of chlorpromazine and the drug was added 2 hpi, the expression levels of HCV proteins E2 and NS3 were only slightly reduced (Fig. 3D), and the number of infected cells was similar to that in control untreated cells (Fig. 3E).

As a control, we assessed the impact of chlorpromazine on the infection of Huh-7 cells by Sendai virus (SeV). SeV is a paramyxovirus which enters by direct fusion at the plasma membrane. To facilitate detection, we used a recombinant SeV expressing GFP (28). Chlorpromazine treatment had no effect on the levels of GFP expression (Fig. 3D) or the number of SeV-infected cells (Fig. 3E). These results indicate that the inhibitory effect of chlorpromazine on HCVcc infection primarily results from an inhibition of an early step of the infection, most probably corresponding to entry.

Taken together, the data obtained with CHC depletion and chlorpromazine treatment indicate that HCVcc entry is dependent on an active pathway of clathrin-mediated endocytosis.

HCVcc infection is pH dependent. Since both HCVpp entry and HCVcc infection assays indicated a functional role for clathrin-mediated endocytosis in HCV entry, we also verified that HCVcc infection is indeed dependent on acidic endosomal pH. Huh-7 cells were pretreated for 30 min, infected for 2 h with HCVcc, and cultured for 30 h in the presence of 50 nM bafilomycin A1 or 20 μM chloroquine. These experimental conditions were chosen because they had a strong inhibitory effect on HCVpp entry in PLC/PRF/5 cells and on BVDV infection in MDBK cells (29). HCVcc infection was quantified by immunoblotting. As shown in Fig. 4A, the cellular levels of both E2 and NS3 at 30 hpi were dramatically reduced in the presence of each inhibitor compared to levels for untreated control cells infected with the same amounts of HCVcc. When the cells were infected and bafilomycin A1 was added to infected cells at 2 hpi, the levels of E2 and NS3 were similar to those in the controls, indicating that the drug had no inhibitory effect on HCVcc infection at a postentry step. In contrast, bafilomycin A1 and chloroquine had no effect on the levels of GFP expression mediated by recombinant SeV infection (Fig. 4A).

HCVcc infection was also scored by immunofluorescence microscopy using anti-E2 and anti-C antibodies. No infected cells were observed in cells pretreated and infected in the presence of 50 nM bafilomycin A1 (Fig. 4B and data not shown). In contrast, cells that were infected with no drug and incubated with 50 nM bafilomycin A1 from 2 hpi up to 30 hpi displayed a percentage of infected cells similar to that of controls. Chloroquine also dramatically reduced the number of infected cells (Fig. 4B). In contrast, neither bafilomycin A1 nor chloroquine treatments had any impact on the number of SeV-infected cells (Fig. 4B).

Together with the results from immunoblot analysis, these results indicate the HCVcc entry is sensitive to agents that neutralize the acidic pH of cellular endosomes.

DISCUSSION

To examine the entry of HCV in target cells, we have used two complementary approaches. First we have developed a new assay based on the use of HCVpp to specifically study early entry steps mediated by HCV envelope glycoproteins. This assay is based on the quantification of retroviral DNA synthesis, which occurs soon after the fusion of the retroviral particle with a cellular membrane (21). Presumably, this assay is only dependent on the entry steps mediated by the heterodimer E1E2 (binding, endocytosis, and fusion) and on the activity of the reverse transcriptase of the HCVpp retroviral core. Second, we made use of the recently developed JFH-1 infectious clone to investigate in parallel the entry pathway of HCVcc in the context of an infectious cycle.

Both assays yielded similar conclusions on the mechanisms of HCV entry. Our results indicate that HCVpp and HCVcc enter cells by clathrin-mediated endocytosis. The partial inhibition observed in cells transfected with CHC siRNA is probably due to the incomplete depletion of clathrin from the cells after siRNA treatment rather than to the existence of an alternative entry pathway for HCV, since a similar behavior was observed for Sindbis virus and VSV-Gpp, two controls for clathrin-mediated viral entry (6, 53). HCVcc infection was also found to be sensitive to agents that interfere with the acidic pH of endosomes. Similar findings on the pH dependency of HCVcc entry were recently reported by Tscherne et al. with a recombinant HCVcc clone expressing luciferase (54). This is consistent with an entry mediated by clathrin-mediated endocytosis, since clathrin-coated vesicles deliver their content into endosomes with an acidic content.

Many other viruses are known to hijack endocytic pathways. The sensitivity to lysosomotropic agents has often been considered evidence for an entry by endocytosis. However, viruses insensitive to lysosomotropic agents may also enter cells by endocytosis (12, 20, 33, 40). Several endocytic pathways were recently identified in addition to the clathrin-mediated pathway (10, 39, 51). These newly discovered pathways differ in the type of vesicular carrier formed at the plasma membrane to carry out the internalization step and also differ in the type of intracellular compartments to which the internalized material is transported. Some of them carry ligands to the classical acidic early and late endosomes, which are also reached by endocytic ligands originating from clathrin-coated vesicles, while other ones deliver their ligands to compartments with neutral pH, such as caveosomes, endoplasmic reticulum, or the Golgi complex (35, 39). Not surprisingly, it appears that viruses have evolved to adapt to these different entry routes. Several enveloped and nonenveloped viruses have been reported to use various alternative endocytic pathways, whether they are sensitive or not to acidic pH. SV40 enters through caveola-mediated internalization in CV-1 cells (40). Echovirus 1 and rotavirus are internalized by clathrin- and caveola-independent pathways, which require dynamin function and are sensitive to the cholesterol-sequestering drug methyl-β-cyclodextrin (41, 47). Lymphocytic choriomeningitis virus is endocytosed into cells by noncoated vesicles and reaches an acidic intracellular compartment where a process of pH-dependent fusion occurs (5). Influenza viruses can be endocytosed both by clathrin-independent and clathrin-dependent mechanisms into the same cell (46, 52).

During experiments involving CHC depletion, we made use of SV40 as a control for clathrin-independent endocytosis. SV40 was recently reported to infect Huh-7 cells by a unique route involving neither clathrin-mediated endocytosis nor the internalization of caveolae, which are absent from Huh-7 cells (12). In Huh-7 cells, the endocytosis of SV40 virions occurs through small uncoated vesicles that are formed at the plasma membrane in a dynamin-independent manner, and they are sensitive to cholesterol-sequestering drugs (12). Interestingly, we found that the depletion of clathrin heavy chain results in an increased SV40 infection, possibly by enhancing its endocytic pathway. It is well established that many regulatory factors have opposite effects on clathrin-mediated and on caveolae/lipid raft-mediated endocytosis (38). We can therefore hypothesize that the inhibition of clathrin-mediated endocytosis might induce compensatory mechanisms up-regulating alternative endocytic pathways in order to control the homoeostasis of the plasma membrane. Similarly, up-regulation of dynamin-independent fluid-phase uptake has been reported in cells expressing dominant-negative dynamin mutants (11).

In the *Flaviviridae* family, the entry of viruses of the *Flavivirus* and *Pestivirus* genera was examined before. Early electron microscopy studies suggested that the flavivirus West Nile virus enters cells through clathrin-coated vesicles (22). This mode of entry was recently confirmed by the use of a dominant-negative form of Eps15 as a way to functionally probe the clathrin-mediated pathway (8). This is consistent with numerous studies which have shown that the envelope glycoprotein E of flaviviruses undergoes a conformational transition under acidic conditions from a native dimeric form to a fusogenic trimeric form (23). Such an acid-triggered conformational transition has not been reported at the present time for the envelope proteins of pestiviruses or HCV.

The pestivirus BVDV also enters by clathrin-mediated endocytosis (26, 29). Consistent with this mode of entry, BVDV infection is sensitive to agents that neutralize the pH of endosomes. However, unlike flaviviruses, BVDV and HCVcc particles are stable and stay infectious when incubated at acidic pH before infection (26, 54). In similar conditions, flaviviruses, alphaviruses, and other enveloped viruses are inactivated, presumably because the pH triggers irreversible conformational changes in the envelope glycoproteins of these viruses similar to those associated with the fusion process during entry. This indicates that a pH drop is not sufficient to induce the conformational changes associated with the fusion process mediated by the envelope glycoproteins of pestiviruses and hepaciviruses, or that the changes in conformation triggered under acidic conditions are reversible in the absence of a cellular membrane. Such reversible conformational changes were reported for VSV (43).

It has been suggested that HCV and BVDV envelope glycoproteins must be primed to acquire a fusogenic conformation triggered by pH. This priming event can be mimicked to some extent by pretreating BVDV particles with reducing agents (26). Under reducing conditions, BVDV virions became pH sensitive, and their fusion to the plasma membrane was inducible at pH 5.

Our study suggests that, like flaviviruses and pestiviruses, HCV enters cells through clathrin-mediated endocytosis and fusion from within an acidic endosomal compartment. At the present time, we still do not know the exact nature of the endosomal compartment that is competent for HCV fusion. We also do not know whether the acidic pH of endosomes acts directly on the conformation of HCV envelope glycoproteins E1 and E2 to trigger fusion or whether it acts indirectly by activating other endosomal agents, which in turn would promote HCV fusion. It would be interesting to determine if HCV fusion requires a priming event to allow an acid-triggered conformational change of the E1E2 heterodimer or if the fusion may be directly induced by a pH drop, as is the case for flaviviruses. Tscherne et al. recently reported that HCVcc infection by direct fusion at the plasma membrane induced by a pH drop was very inefficient (54). However, it is not known if the blockade was at the fusion step or at a postfusion step. On the other hand, experiments carried out in vitro with HCVpp indicated that fusion to liposomes mediated by HCV E1E2 heterodimer is readily inducible at acidic pH (27). This suggests that a preliminary priming event would not be necessary for HCV E1E2-mediated fusion. It remains to be determined if conformational changes in E1E2 are associated with the fusion process and if similar findings are observed with HCVcc particles. Such questions could be addressed once it becomes possible to purify HCVcc particles for in vitro studies.

ACKNOWLEDGMENTS

We thank Laetitia Corset and Anne Goffard for help with real-time PCR. We are grateful to J. F. Delagneau, A. Patel, and J. McKeating for providing us with antibodies, D. Lavillette and F.-L. Cosset for plasmids, and L. Roux and F. Lafont for the purified stock of SeV. Some data were generated with the help of the Imaging Core Facility of the Calmette campus.

This work was supported by a grant from the "Agence Nationale de Recherche sur le Sida et les Hépatites Virales" (ANRS) to Y.R. and C.W.E.B. was supported by a postdoctoral fellowship from the ANRS. T.W. was partly supported by a grant from the Ministry of Health, Labor, and Welfare of Japan, the Program for Promotion of Fundamental Studies in Health Sciences of the National Institute of Biomedical Innovation (NIBIO), and Research on Health Sciences focusing on Drug Innovation from the Japan Health Sciences Foundation. J.D. is an international scholar of the Howard Hughes Medical Institute.

REFERENCES

1. **Agnello, V., G. Ábel, M. Elfahal, G. B. Knight, and Q. X. Zhang.** 1999. Hepatitis C virus and other flaviviridae viruses enter cells via low density lipoprotein receptor. Proc. Natl. Acad. Sci. USA **96**:12766–12771.
2. **Barth, H., C. Schäfer, M. I. Adah, F. Zhang, R. J. Linhardt, H. Toyoda, A. Kinoshita-Toyoda, T. Toida, T. H. Van Kuppevelt, E. Depla, F. Von Weizsacker, H. E. Blum, and T. F. Baumert.** 2003. Cellular binding of hepatitis C virus envelope glycoprotein E2 requires cell surface heparan sulfate. J. Biol. Chem. **278**:41003–41012.
3. **Bartosch, B., J. Dubuisson, and F.-L. Cosset.** 2003. Infectious hepatitis C virus pseudo-particles containing functional E1–E2 envelope protein complexes. J. Exp. Med. **197**:633–642.
4. **Bartosch, B., A. Vitelli, C. Granier, C. Goujon, J. Dubuisson, S. Pascale, E. Scarselli, R. Cortese, A. Nicosia, and F.-L. Cosset.** 2003. Cell entry of hepatitis C virus requires a set of co-receptors that include the CD81 tetraspanin and the SR-B1 scavenger receptor. J. Biol. Chem. **278**:41624–41630.
5. **Borrow, P., and M. B. Oldstone.** 1994. Mechanism of lymphocytic choriomeningitis virus entry into cells. Virology **198**:1–9.
6. **Carbone, R., S. Fre, G. Iannolo, F. Belleudi, P. Mancini, P. G. Pelicci, M. R. Torrisi, and P. P. Di Fiore.** 1997. eps15 and eps15R are essential components of the endocytic pathway. Cancer Res. **57**:5498–5504.
7. **Choo, Q. L., G. Kuo, A. J. Weiner, L. R. Overby, D. W. Bradley, and M. Houghton.** 1989. Isolation of a cDNA clone derived from a blood-borne non-A, non-B viral hepatitis genome. Science **244**:359–362.
8. **Chu, J. J., and M. L. Ng.** 2004. Infectious entry of West Nile virus occurs through a clathrin-mediated endocytic pathway. J. Virol. **78**:10543–10555.
9. **Clayton, R. F., A. Owsianka, J. Aitken, S. Graham, D. Bhella, and A. H. Patel.** 2002. Analysis of antigenicity and topology of E2 glycoprotein present on recombinant hepatitis C virus-like particles. J. Virol. **76**:7672–7682.
10. **Conner, S. D., and S. L. Schmid.** 2003. Regulated portals of entry into the cell. Nature **422**:37–44.
11. **Damke, H., T. Baba, A. M. van der Bliek, and S. L. Schmid.** 1995. Clathrin-independent pinocytosis is induced in cells overexpressing a temperature-sensitive mutant of dynamin. J. Cell Biol. **131**:69–80.
12. **Damm, E. M., L. Pelkmans, J. Kartenbeck, A. Mezzacasa, T. Kurzchalia, and A. Helenius.** 2005. Clathrin- and caveolin-1-independent endocytosis: entry of simian virus 40 into cells devoid of caveolae. J. Cell Biol. **168**:477–488.
13. **Deleersnyder, V., A. Pillez, C. Wychowski, K. Blight, J. Xu, Y. S. Hahn, C. M. Rice, and J. Dubuisson.** 1997. Formation of native hepatitis C virus glycoprotein complexes. J. Virol. **71**:697–704.
14. **Drummer, H. E., A. Maerz, and P. Poumbourios.** 2003. Cell surface expression of functional hepatitis C virus E1 and E2 glycoproteins. FEBS Lett. **546**:385–390.
15. **Dubuisson, J., H. H. Hsu, R. C. Cheung, H. B. Greenberg, D. G. Russell, and C. M. Rice.** 1994. Formation and intracellular localization of hepatitis C virus envelope glycoprotein complexes expressed by recombinant vaccinia and Sindbis viruses. J. Virol. **68**:6147–6160.
16. **Duvet, S., F. Chirat, A. M. Mir, A. Verbert, J. Dubuisson, and R. Cacan.** 2000. Reciprocal relationship between alpha1,2 mannosidase processing and reglucosylation in the rough endoplasmic reticulum of Man-P-Dol deficient cells. Eur. J. Biochem. **267**:1146–1152.
17. **Flint, M., C. Maidens, L. D. Loomis-Price, C. Shotton, J. Dubuisson, P. Monk, A. Higginbottom, S. Levy, and J. A. McKeating.** 1999. Characterization of hepatitis C virus E2 glycoprotein interaction with a putative cellular receptor, CD81. J. Virol. **73**:6235–6244.
18. **Gardner, J. P., R. J. Durso, R. R. Arrigale, G. P. Donovan, P. J. Maddon, T. Dragic, and W. C. Olson.** 2003. L-SIGN (CD 209L) is a liver-specific capture receptor for hepatitis C virus. Proc. Natl. Acad. Sci. USA **100**:4498–4503.
19. **Gault, E., Y. Michel, A. Dehée, C. Belabani, J. C. Nicolas, and A. Garbarg-Chenon.** 2001. Quantification of human cytomegalovirus DNA by real-time PCR. J. Clin. Microbiol. **39**:772–775.
20. **Gianni, T., G. Campadelli-Fiume, and L. Menotti.** 2004. Entry of herpes simplex virus mediated by chimeric forms of nectin1 retargeted to endosomes or to lipid rafts occurs through acidic endosomes. J. Virol. **78**:12268–12276.
21. **Goff, S. P.** 2001. *Retroviridae*: The retroviruses and their replication, p. 1871–1940. *In* D. M. Knipe and P. M. Howley (ed.), Fields virology, 4th ed., vol. 2. Lippincott, Williams & Wilkins, Philadelphia, Pa.
22. **Gollins, S. W., and J. S. Porterfield.** 1985. Flavivirus infection enhancement in macrophages: an electron microscopic study of viral cellular entry. J. Gen. Virol. **66**:1969–1982.
23. **Heinz, F. X., K. Stiasny, and S. L. Allison.** 2004. The entry machinery of flaviviruses. Arch. Virol. Suppl. **2004**:133–137.
24. **Hsu, M., J. Zhang, M. Flint, C. Logvinoff, C. Cheng-Mayer, C. M. Rice, and J. A. McKeating.** 2003. Hepatitis C virus glycoproteins mediate pH-dependent cell entry of pseudotyped retroviral particles. Proc. Natl. Acad. Sci. USA **100**:7271–7276.
25. **Kato, T., T. Date, M. Miyamoto, A. Furusaka, K. Tokushige, M. Mizokami, and T. Wakita.** 2003. Efficient replication of the genotype 2a hepatitis C virus subgenomic replicon. Gastroenterology **125**:1808–1817.
26. **Krey, T., H. J. Thiel, and T. Rümenapf.** 2005. Acid-resistant bovine pestivirus requires activation for pH-triggered fusion during entry. J. Virol. **79**:4191–4200.
27. **Lavillette, D., B. Bartosch, D. Nourrisson, G. Verney, F.-L. Cosset, F. Penin, and E. I. Pécheur.** 2006. Hepatitis C virus glycoproteins mediate low pH-dependent membrane fusion with liposomes. J. Biol. Chem. **281**:3909–3917.
28. **Le Mercier, P., D. Garcin, S. Hausmann, and D. Kolakofsky.** 2002. Ambisense Sendai viruses are inherently unstable but are useful to study viral RNA synthesis. J. Virol. **76**:5492–5502.
29. **Lecot, S., S. Belouzard, J. Dubuisson, and Y. Rouillé.** 2005. Bovine viral diarrhea virus entry is dependent on clathrin-mediated endocytosis. J. Virol. **79**:10826–10829.
30. **Lindenbach, B. D., M. J. Evans, A. J. Syder, B. Wölk, T. L. Tellinghuisen, C. C. Liu, T. Maruyama, R. O. Hynes, D. R. Burton, J. A. McKeating, and C. M. Rice.** 2005. Complete replication of hepatitis C virus in cell culture. Science **309**:623–626.
31. **Lindenbach, B. D., and C. M. Rice.** 2001. *Flaviviridae*: The viruses and their replication, p. 991–1042. *In* D. M. Knipe and P. M. Howley (ed.), Fields virology, 4th ed., vol. 1. Lippincott, Williams & Wilkins, Philadelphia, Pa.
32. **Lozach, P. Y., H. Lortat-Jacob, A. de Lacroix de Lavalette, I. Staropoli, S. Foung, A. Amara, C. Houlès, F. Fieschi, O. Schwartz, J.-L. Virelizier, F. Arenzana-Seisdedos, and R. Altmeyer.** 2003. DC-SIGN and L-SIGN are high affinity binding receptors for hepatitis C virus glycoprotein E2. J. Biol. Chem. **278**:20358–20366.
33. **Mothes, W., A. L. Boerger, S. Narayan, J. M. Cunningham, and J. A. Young.** 2000. Retroviral entry mediated by receptor priming and low pH triggering of an envelope glycoprotein. Cell **103**:679–689.
34. **Motley, A., N. A. Bright, M. N. Seaman, and M. S. Robinson.** 2003. Clathrin-mediated endocytosis in AP-2-depleted cells. J. Cell Biol. **162**:909–918.
35. **Nichols, B.** 2003. Caveosomes and endocytosis of lipid rafts. J. Cell Sci. **116**:4707–4714.
36. **O'Doherty, U., W. J. Swiggard, and M. H. Malim.** 2000. Human immunodeficiency virus type 1 spinoculation enhances infection through virus binding. J. Virol. **74**:10074–10080.
37. **Op De Beeck, A., C. Voisset, B. Bartosch, Y. Ciczora, L. Cocquerel, Z. Keck, S. Foung, F.-L. Cosset, and J. Dubuisson.** 2004. Characterization of functional hepatitis C virus envelope glycoproteins. J. Virol. **78**:2994–3002.
38. **Pelkmans, L., E. Fava, H. Grabner, M. Hannus, B. Habermann, E. Krausz, and M. Zerial.** 2005. Genome-wide analysis of human kinases in clathrin- and caveolae/raft-mediated endocytosis. Nature **436**:78–86.
39. **Pelkmans, L., and A. Helenius.** 2003. Insider information: what viruses tell us about endocytosis. Curr. Opin. Cell Biol. **15**:414–422.
40. **Pelkmans, L., J. Kartenbeck, and A. Helenius.** 2001. Caveolar endocytosis of simian virus 40 reveals a new two-step vesicular-transport pathway to the ER. Nat. Cell Biol. **3**:473–483.
41. **Pietiäinen, V., V. Marjomäki, P. Upla, L. Pelkmans, A. Helenius, and T. Hyypiä.** 2004. Echovirus 1 endocytosis into caveosomes requires lipid rafts, dynamin II, and signaling events. Mol. Biol. Cell **15**:4911–4925.
42. **Pileri, P., Y. Uematsu, S. Campagnoli, G. Galli, F. Falugi, R. Petracca, A. J. Weiner, M. Houghton, D. Rosa, G. Grandi, and S. Abrignani.** 1998. Binding of hepatitis C virus to CD81. Science **282**:938–941.
43. **Puri, A., J. Winick, R. J. Lowy, D. Covell, O. Eidelman, A. Walter, and R. Blumenthal.** 1988. Activation of vesicular stomatitis virus fusion with cells by pretreatment at low pH. J. Biol. Chem. **263**:4749–4753.
44. **Rouillé, Y., F. Helle, D. Delgrange, P. Roingeard, C. Voisset, E. Blanchard, S. Belouzard, J. McKeating, A. H. Patel, G. Maertens, T. Wakita, C. Wychowski, and J. Dubuisson.** 2006. Subcellular localization of hepatitis C virus structural proteins in a cell culture system that efficiently replicates the virus. J. Virol. **80**:2832–2841.
45. **Rozen, S., and H. J. Skaletsky.** 2000. Primer3 on the WWW for general users and for biologist programmers, p. 365–386. *In* S. Krawetz and S. Misener (ed.), Bioinformatics methods and protocols: methods in molecular biology. Humana Press, Totowa, N.J.
46. **Rust, M. J., M. Lakadamyali, F. Zhang, and X. Zhuang.** 2004. Assembly of endocytic machinery around individual influenza viruses during viral entry. Nat. Struct. Mol. Biol. **11**:567–573.
47. **Sánchez-San Martín, C., T. López, C. F. Arias, and S. López.** 2004. Characterization of rotavirus cell entry. J. Virol. **78**:2310–2318.
48. **Sandrin, V., and F. L. Cosset.** 2006. Intracellular versus cell surface assembly of retroviral pseudotypes is determined by the cellular localization of the

viral glycoprotein, its capacity to interact with Gag and the expression of the Nef protein. J. Biol. Chem. 281:528–542.
49. **Saunier, B., M. Triyatni, L. Ulianich, P. Maruvada, P. Yen, and L. D. Kohn.** 2003. Role of the asialoglycoprotein receptor in binding and entry of hepatitis C virus structural proteins in cultured human hepatocytes. J. Virol. 77:546–559.
50. **Scarselli, E., H. Ansuini, R. Cerino, R. M. Roccasecca, S. Acali, G. Filocamo, C. Traboni, A. Nicosia, R. Cortese, and A. Vitelli.** 2002. The human scavenger receptor class B type I is a novel candidate receptor for the hepatitis C virus. EMBO J. 21:5017–5025.
51. **Sieczkarski, S. B., and G. R. Whittaker.** 2002. Dissecting virus entry via endocytosis. J. Gen. Virol. 83:1535–1545.
52. **Sieczkarski, S. B., and G. R. Whittaker.** 2002. Influenza virus can enter and infect cells in the absence of clathrin-mediated endocytosis. J. Virol. 76: 10455–10464.
53. **Sun, X., V. K. Yau, B. J. Briggs, and G. R. Whittaker.** 2005. Role of clathrin-mediated endocytosis during vesicular stomatitis virus entry into host cells. Virology 338:53–60.
54. **Tscherne, D. M., C. T. Jones, M. J. Evans, B. D. Lindenbach, J. A. McKeating, and C. M. Rice.** 2006. Time- and temperature-dependent activation of hepatitis C virus for low-pH-triggered entry. J. Virol. 80:1734–1741.
55. **Voisset, C., N. Callens, E. Blanchard, A. Op De Beeck, J. Dubuisson, and N. Vu-Dac.** 2005. High density lipoproteins facilitate hepatitis C virus entry through the scavenger receptor class B type I. J. Biol. Chem. 280:7793–7799.
56. **Wakita, T., T. Pietschmann, T. Kato, T. Date, M. Miyamoto, Z. Zhao, K. Murthy, A. Habermann, H. G. Krausslich, M. Mizokami, R. Bartenschlager, and T. J. Liang.** 2005. Production of infectious hepatitis C virus in tissue culture from a cloned viral genome. Nat. Med. 11:791–796.
57. **Wang, L. H., K. G. Rothberg, and R. G. Anderson.** 1993. Mis-assembly of clathrin lattices on endosomes reveals a regulatory switch for coated pit formation. J. Cell Biol. 123:1107–1117.
58. **Wychowski, C., D. Benichou, and M. Girard.** 1986. A domain of SV40 capsid polypeptide VP1 that specifies migration into the cell nucleus. EMBO J. 5:2569–2576.
59. **Zhong, J., P. Gastaminza, G. Cheng, S. Kapadia, T. Kato, D. R. Burton, S. F. Wieland, S. L. Uprichard, T. Wakita, and F. V. Chisari.** 2005. Robust hepatitis C virus infection in vitro. Proc. Natl. Acad. Sci. USA 102:9294–9299.

JOURNAL OF VIROLOGY, May 2006, p. 4633–4639 Vol. 80, No. 9
0022-538X/06/$08.00+0 doi:10.1128/JVI.80.9.4633–4639.2006

NOTE

Generation of Infectious Hepatitis C Virus in Immortalized Human Hepatocytes

Tatsuo Kanda,[1]† Arnab Basu,[2]† Robert Steele,[1] Takaji Wakita,[4] Jan S. Ryerse,[1] Ranjit Ray,[2,3]* and Ratna B. Ray[1,2]*

Departments of Pathology,[1] Internal Medicine,[2] and Molecular Microbiology and Immunology,[3] Saint Louis University, St. Louis, Missouri 63110, and Department of Microbiology, Tokyo Metropolitan Institute for Neuroscience, Tokyo 183-8526, Japan[4]

Received 15 November 2005/Accepted 12 February 2006

Progress in understanding hepatitis C virus (HCV) biology has remained a challenge due to the lack of an efficient cell culture system for virus growth. In this study, we examined HCV core protein-mediated immortalized human hepatocytes (IHH) for growth of HCV. In vitro-transcribed full-length RNA from HCV genotype 1a (clone H77) was introduced into IHH by electroporation. Reverse transcription-PCR of cellular RNA isolated from HCV genome-transfected IHH suggested that viral RNA replication occurred. IHH transfected with the full-length HCV genome also displayed viral protein expression by indirect immunofluorescence. In contrast, cells transfected with polymerase-defective HCV (H77/GND) RNA as a negative control did not exhibit expression of the viral genome. Immunogold labeling demonstrated localization of E1 protein in the rough endoplasmic reticulum of RNA-transfected IHH. Virus-like particles of ~50 nm were observed in the cytoplasm. After being inoculated with culture media of cells transfected with the full-length HCV genome, naïve IHH displayed NS5a protein expression in a dilution-dependent manner, but expression of NS5a was inhibited by prior incubation of culture medium with HCV-infected patient sera. NS5a-positive immunofluorescence of cell culture media of IHH transfected with full-length H77 RNA yielded ~4.5×10^4 to 1×10^5 focus-forming units/ml. A similar level of virus growth was observed upon transfection of RNA from HCV genotype 2a (JFH1) into IHH. Taken together, our results suggest that IHH support HCV genome replication and virus assembly.

Hepatitis C virus (HCV) is an important cause of morbidity and mortality worldwide. The most important feature of HCV infection is the development of chronic hepatitis in a significant number of infected individuals, with the potential for disease progression to cirrhosis and hepatocellular carcinoma (6, 7, 11, 27). At present, the only approved therapies for chronic HCV infection are alpha interferon (IFN-α) with or without ribavirin (9, 21), but these fail to clear HCV from a significant number of patients (22). A number of HCV genomes have been cloned, and sequence divergence indicates that there are several genotypes and a series of subtypes of this virus (28). In the United States, HCV genotypes 1a and 1b are predominant in patients with chronic hepatitis C (32). Progress in understanding HCV biology has remained challenging due to the lack of an efficient cell culture system for virus growth. Establishment of self-replicating full-length HCV genomic replicons from genotypes 1a and 1b in human hepatoma (Huh-7) cells has provided an important tool for the study of HCV replication mechanisms (3, 10, 23). Recently, different groups have reported the generation of infectious virus from transfection of genomic RNA of HCV genotype 2a into Huh-7 cells or its derivatives (5, 15, 29, 33). However, generation of infectious HCV genotype 1a has not been successful to date.

We and others have shown that HCV core protein transcriptionally regulates a number of cellular genes (26). We previously described the generation of immortalized human hepatocytes (IHH) by transfection of the HCV core genomic region from genotype 1a (2, 25). IHH exhibited a weak level of HCV core protein expression, albumin secretion, glucose phosphatase activity, and absence of smooth-muscle actin. IHH also displayed focal cytoplasmic and membrane staining for carcinoembryonic antigen (CEA), biliary glycoprotein (BGP1/CEACAM1), and nonspecific cross-reacting antigen (NCA/CEACAM6) and expression of hepato-biliary transport marker genes (MRP, LST1, and NTCP) (unpublished observations). Together, these results suggested that IHH are well differentiated. HCV core protein selectively degrades STAT1, reduces phosphorylated STAT1 accumulation in the nucleus in a proteasome-dependent manner, and impairs IFN-α-induced signal transduction via expression of suppressor of cytokine signaling-3 (1, 4, 16, 18). HCV core protein is competent to partially rescue growth of a genetically engineered influenza A virus lacking its own IFN antagonist (4). The core protein can modulate interferon regulatory factor, Jak-STAT, and inducible nitric oxide synthetase pathways, which suggests that there are mechanisms by which the core could affect HCV persistence and pathogenesis (20). Since HCV core protein transcriptionally regulates several cellular genes involved in cell growth, apoptosis, and defense mech-

* Corresponding author. Mailing address: Saint Louis University, 3635 Vista Avenue, St. Louis, MO 63110. Phone: (314) 577-8648. Fax: (314) 771-3816. E-mail for Ranjit Ray: rayr@slu.edu. E-mail for Ratna B. Ray: rayrb@slu.edu.

† T.K. and A.B. contributed equally to this study.

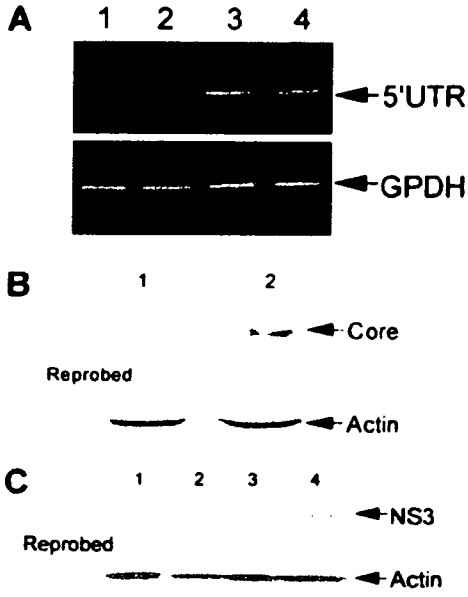

FIG. 1. HCV RNA and protein expression in IHH. (A) RT-PCR analysis was performed using 5'UTR-specific primers from RNA isolated at day 5 from two different sets of IHH transfected with H77/GND RNA as a negative control (lanes 1 and 2) or H77 RNA (lanes 3 and 4). GPDH was amplified as an internal control. The sizes of the amplified bands were verified from the migration of a φX174-HaeIII digested DNA marker (not shown). (B) Western blot analysis for core protein expression in H77/GND RNA-transfected (lane 1) and H77 RNA-transfected (lane 2) IHH, using a specific antiserum. The blot was reprobed with antibody to actin for similar protein loads in each lane. (C) Western blot analysis for NS3 protein expression in two different sets of IHH transfected with H77/GND RNA (lanes 1 and 2) or H77 RNA (lanes 3 and 4), using a specific monoclonal antibody. The blot was reprobed with antibody to actin for similar protein loads in each lane. The molecular weights of the protein bands were verified from the migration of protein molecular weight markers (Cambrex, Rockland, Maine).

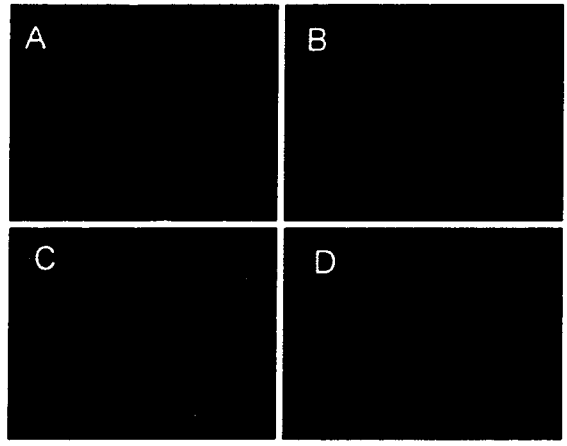

FIG. 2. Intracellular expression of HCV proteins. IHH transfected with RNA from the H77 clone (A) or the negative control, H77/GND (B), were treated with an NS5a-specific monoclonal antibody for detection of protein expression by intracellular immunofluorescence 5 days after transfection. IHH were similarly transfected with RNA from the JFH1 clone (C) or the negative control, JFH1/GND (D), and treated with a specific monoclonal antibody for intracellular localization of NS3. Green indicates NS5a staining, and red indicates NS3 staining.

anisms, we hypothesize that IHH may set the stage for HCV genome replication and assembly.

(Part of this study was presented at the International Congress of Virology, IUMS, San Francisco, Calif., 2005, and the 12th International Symposium on Hepatitis C Virus and Related Viruses, Montreal, Canada, 2005.)

Replication of the HCV genome and virus protein expression. We investigated whether IHH confer HCV genome replication and generation of infectious virus particles. For this purpose, full-length RNAs from HCV genotype 1a (clone H77) (13) were used. The clone H77 contains a 5′ untranslated region (5′UTR), a coding sequence, and a 3′UTR, which are suggested to be necessary for replication (14, 30). In vitro-transcribed full-length HCV RNA from clone H77 was used for transfection of IHH by electroporation. H77/GND (polymerase-defective) RNA was used similarly as a negative control. Briefly, H77 cDNA was linearized by digestion with XbaI, and gel-purified DNA was used for in vitro transcription by T7 RNA polymerase (Promega, Madison, Wis.). In vitro-transcribed RNA (1 to 2 μg) was introduced by electroporation (950 μF and 270 V) into 5×10^6 IHH, using a Bio-Rad Gene Pulser Xcell system (Hercules, Calif.). The transfected cells were plated on collagen-coated plastic dishes and maintained in culture for HCV replication. Total cellular RNA was extracted 5 days posttransfection. To detect the HCV genome, total cellular RNA and random hexamers were used for cDNA synthesis with a SuperScriptIII first-strand-synthesis system (Invitrogen), following the supplier's protocol. PCR amplification was performed with cDNA as a template, using sense (5′-CACTCCCCTGTGAGGAACTACTGTCT-3′) and antisense (5′-TGGTGCACGGTCTACGAGACCTCCC-3′) primers from 5′UTR at 94°C for 30 s, annealing at 55°C for 60 s, and extension at 72°C for 90 s. Glyceraldehyde-3-phosphate dehydrogenase (GPDH) was used as an internal control, using specific primers (17). Reverse transcription-PCR (RT-PCR) analyses suggested amplification of sequence from the 5′UTR (Fig. 1A). In contrast, cells transfected with H77/GND RNA did not exhibit the presence of the HCV genomic sequence. To rule out the integration of H77 plasmid DNA into IHH, genomic DNA from the cell lines was isolated and examined for the HCV genome by PCR. Our results suggested that the HCV sequence was absent, indicating HCV genomic RNA replication occurred in the cytoplasm of IHH (data not shown). Filtered culture supernatant was also treated with RNaseA prior to isolation of viral RNA. RT-PCR was performed for the NS5A region (17), and we observed amplification of a specific RNA sequence.

Western blot analysis using specific antibodies was performed to analyze the expression of core and NS3 proteins in control and experimental cells. Equal amounts of proteins from whole-cell lysates in sample buffer were separated by sodium dodecyl sulfate-polyacrylamide gel electrophoresis. The proteins were transferred onto nitrocellulose, incubated with specific antibodies, and detected by chemiluminescence (Amersham, Piscataway, N.J.). HCV core protein was detected by a specific rabbit antiserum, and NS3 was detected by a

specific mouse monoclonal antibody (ViroGen, Watertown, Mass.). The blots were stripped and reprobed, using a mouse monoclonal antibody to actin (Oncogene Science, Cambridge, Mass.). IHH that supported HCV genome replication displayed the presence of core (~21 kDa) and NS3 (~63 kDa) proteins (Fig. 1B and C). On the other hand, IHH transfected with H77/GND RNA did not show a detectable level of core or NS3 proteins. A weak level of core protein was detected in this set of IHH for immortalization by HCV core protein (Fig. 1B). IHH transfected with HCV full-length RNA were passaged at 4- or 5-day intervals. HCV RNA and protein expression were detected in cell cultures for up to 12 days, and the cultures were discontinued for lack of growth after 2 weeks.

To further examine intracellular expression of HCV protein, IHH transfected with H77 RNA were fixed with 3.7% formaldehyde and incubated at room temperature for 1 h with monoclonal antibodies to NS5a (Biogenesis, Kingstone, N.H.). Cells were washed three times with phosphate-buffered saline (PBS), stained with anti-mouse immunoglobulin (Ig) conjugated with Alexa 568 (Molecular Probes, Eugene, Oreg.), and mounted for fluorescence microscopy. Primary antibodies and secondary antibody-fluorochrome conjugates were titrated for use of optimum dilutions where there was no background fluorescence. We observed cytoplasmic expression of NS5a (Fig. 2A) in 60% IHH after 5 days of transfection. HCV genotype 2a (clone JFH1) has been shown to grow in Huh-7 cells or its derivatives (5, 12, 15, 29, 33). In vitro-transcribed RNA from clone JFH1 was used for transfection of IHH to determine if the immortalized hepatocyte cell line supports HCV growth. Intracellular localization of NS3 protein from JFH1 RNA-transfected IHH was detected by immunofluorescence (Fig. 2C). We have also used Huh-7.5 cells transfected with JFH1 RNA as positive controls (29) and observed NS3 expression by indirect immunofluorescence (data not shown). On the other hand, IHH similarly transfected with RNA from H77/GND or the JFH1/GND clone did not display virus protein expression by immunofluorescence (Fig. 2B and D).

Immunogold localization of virus-like particles. Phase-contrast microscopy suggested that HCV genome-transfected IHH were swollen with large vacuoles in the cytoplasm, whereas the negative controls did not show any detectable changes. We also looked for cellular changes, using electron microscopy, and at the ultrastructural level some of these vacuoles appeared to be empty (Fig. 3A and E). Others contained lipid (Fig. 3E) or material isolated for degradation (Fig. 3D). Ultrastructural changes also included increased polymorphism of the nuclei (Fig. 3E). Immunogold labeling was performed for localization of HCV-like particles in transfected IHH. For this, transfected IHH (4 days in culture) were detached from collagen-coated petri dishes by a brief trypsin treatment, pelleted in a microcentrifuge, and fixed in 4% paraformaldehyde and 1% glutaraldehyde in PBS for 16 h at 4°C. After being washed with PBS, the cells were washed in distilled water, dehydrated in ethanol, and infiltrated with LR White resin (London Resin Company, Berkshire, United Kingdom). The cell pellets were polymerized in BEEM capsules (Ted Pella, Inc., Redding, Calif.) at −20°C under UV light. Thin sections were cut from blocks, collected on Formvar-coated nickel grids, and blocked with 1% fish gelatin and 1% bovine serum albumin (BSA) in PBS for 10 min. Sections were incubated for 2 h in a 1:100 dilution (titrated beforehand for best results) of monoclonal antibody to E1 glycoprotein (305/C3) or normal mouse IgG in PBS containing 0.1% BSA, washed in PBS containing 0.1% BSA, and incubated for 1 h in protein A-10-nm colloidal gold (CG) diluted at a ratio of 1:200 in PBS containing 0.1% BSA. After being washed with PBS, the grids were fixed for 3 min in glutaraldehyde, washed in distilled water, stained with uranyl acetate and lead citrate, and photographed with a JEOL 100 CX electron microscope. No clusters of CG particles were observed in the controls, which were stained with normal mouse IgG without the primary antibody or were mock-transfected and stained with the 305/C3 monoclonal antibody. Several hundred cells were evaluated in each case. Immunogold labeling with E1-specific monoclonal antibody demonstrated the presence of HCV-like particles and E1 protein in IHH. Numerous labeled virus-like particles were observed in the cytoplasm (Fig. 3A and E) and near the plasma membrane (Fig. 3C) of H77 RNA-transfected IHH. The labeled particles were ~50 nm in diameter. Extensive labeling was also associated with the rough endoplasmic reticulum, consistent with the synthesis of E1 viral protein (Fig. 3B). In addition, we observed cytoplasmic autophagic vacuoles which contained gold-labeled virus-like particles (Fig. 3D).

Processing of cells into LR White resin for immunogold localization omits the conventional osmium tetroxide fixation step to preserve antigenicity but results in reduced tissue contrast. In addition, the identification of virus particles by immunogold labeling at the ultrastructural level can be tricky. For this, we carried out a series of control experiments to ensure labeling specificity. First, we observed clusters of CG on virus-like particles and single CG particles in the endoplasmic reticulum in several independent anti-E1-labeling experiments. Second, H77/GND RNA-transfected IHH (negative controls) showed no such clusters of CG in the cytoplasm or single CG particles localized along the endoplasmic reticulum or membranes (Fig. 3F). Third, incubation of sections of HCV genome-transfected IHH with normal mouse IgG at IgG concentrations similar to those used for the anti-E1 antibody did not result in any specific immunogold labeling. Fourth, omitting anti-E1 antibody did not result in any specific immunogold labeling. Finally, CG particles in the anti-E1-labeling experiments were primarily confined to cells and were not observed to any degree in the spaces around cells, again suggesting the labeling was specific for E1 protein in cells. Thus, the appearance of virus-like particles in RNA-transfected IHH indicated that HCV 1a replicates and assembles as virus particles.

Infection of IHH by HCV from culture medium. We next examined the presence of HCV in IHH cell culture medium. On different days after transfection, culture medium was filtered through a 0.45-μm cellulose acetate membrane (Millipore, Bedford, Mass.), concentrated to ~10- to 20-fold by Millipore ultrafiltration (100-kDa cut off), and used for detection of the HCV genomic sequence by RT-PCR (Fig. 4A). The presence of HCV 5′UTR was detected in culture medium from HCV genome-transfected IHH but not from polymerase-defective HCV RNA-transfected IHH. We obtained ~1.1×10^8 genome copies/ml of culture medium using real-time RT-PCR, as described recently (33). Culture supernatant collected for up to 7 days suggested that the peak HCV genome copy number occurred between 4 and 5 days after transfection.

Next, we determined whether the culture medium contained infectious HCV. For this, culture media was serially twofold

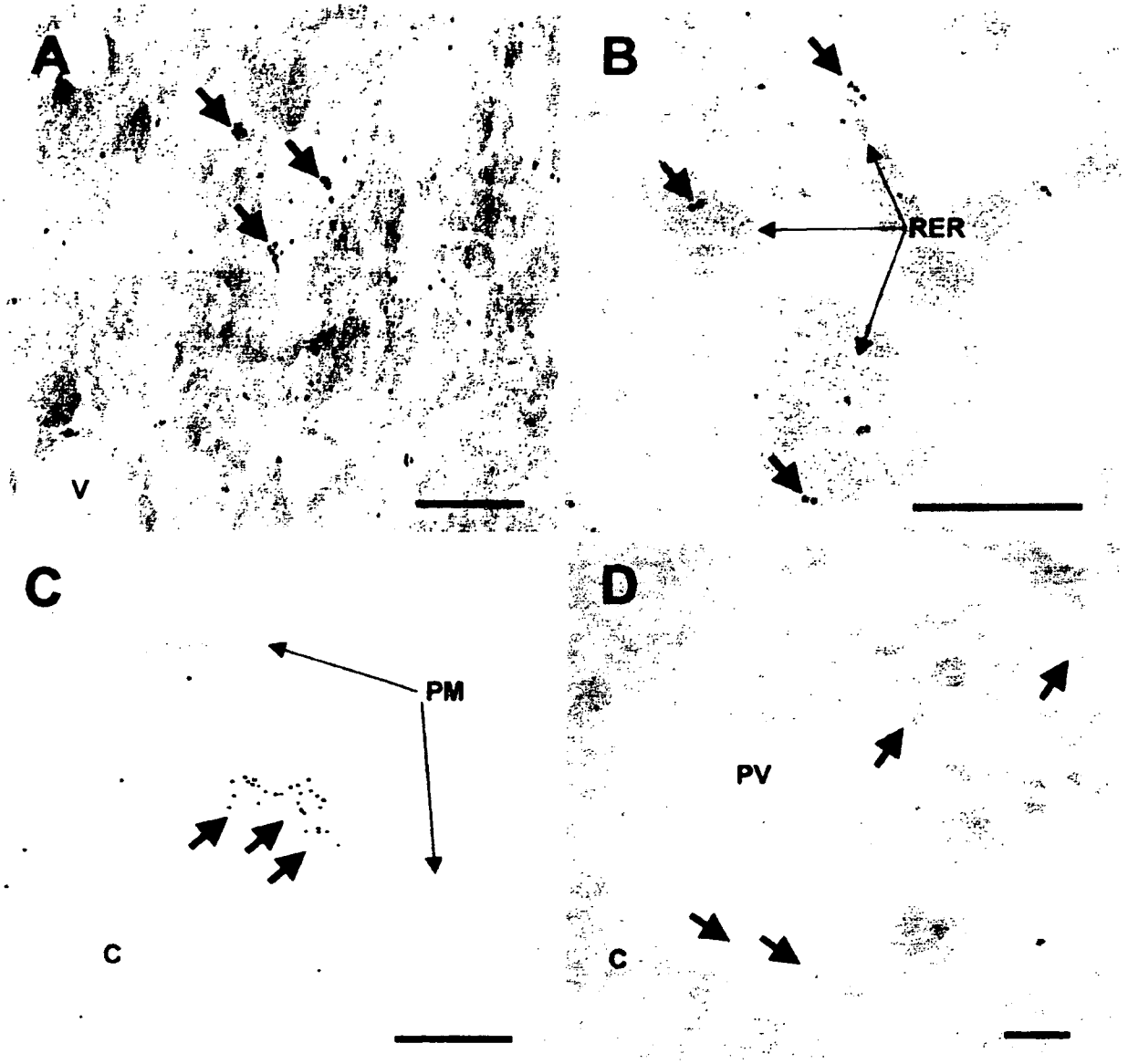

FIG. 3. Immunogold localization of HCV E1 protein and virus-like particles in IHH with a specific monoclonal antibody. (A) Localization of virus-like particles in the cytoplasm is indicated by arrows. (B) Localization of HCV E1 protein to the rough endoplasmic reticulum is marked by arrows. (C) Localization of virus-like particles in the cortical cytoplasm adjacent to the plasma membrane is indicated by arrows. (D) Localization of virus-like particles in a large vacuole in the cytoplasm of IHH is shown by arrows. (E) Clusters of CG indicated by arrows show virus-like particles in IHH. The labeled particle indicated by an arrow and an asterisk is shown at higher magnification in the inset. As observed by light microscopy, IHH contain cytoplasmic vacuoles and lipid droplets. (F) An H77/GND RNA-transfected control section of IHH incubated with monoclonal antibody to E1 glycoprotein did not exhibit immunogold labeling. Other negative controls were labeled with normal mouse IgG and were not incubated with the primary antibody (not shown). Abbreviations: C, cytoplasm; M, mitochondrion; PM, plasma membrane; RER, rough endoplasmic reticulum; V, vacuole; LD, lipid droplet; PV, autophagic vacuole. Magnification bars are 0.25 μm in panels A through F and 0.1 μm in the inset in panel E.

diluted and inoculated into naïve IHH. Cells were incubated for 4 h, washed, and incubated with fresh media for 3 days before indirect immunofluorescence was performed to determine the number of focus-forming units (FFU)/ml of NS5a (H77 clone) or NS3 (JFH1 clone), as recently described (33). Nuclear staining was performed using TO-PRO3-iodide (Molecular Probes), and cells were mounted for confocal laser scanning microscopy (model 1024; Bio-Rad). Figure 4B shows infection of IHH by H77 or JFH1 and is representative of our results. Fluorescent cells were counted, and the counts were correlated with the number of dilutions of cell culture media to determine FFU/ml of H77 and JFH1 clones. We observed ~4.5×10^4 to 1×10^5 FFU/ml of H77 and JFH1 clones in the cell culture media 5 days after transfection.

We transfected in vitro-transcribed H77 or JFH1 RNA into IHH and isolated the RNA from the transfected cells. Culture

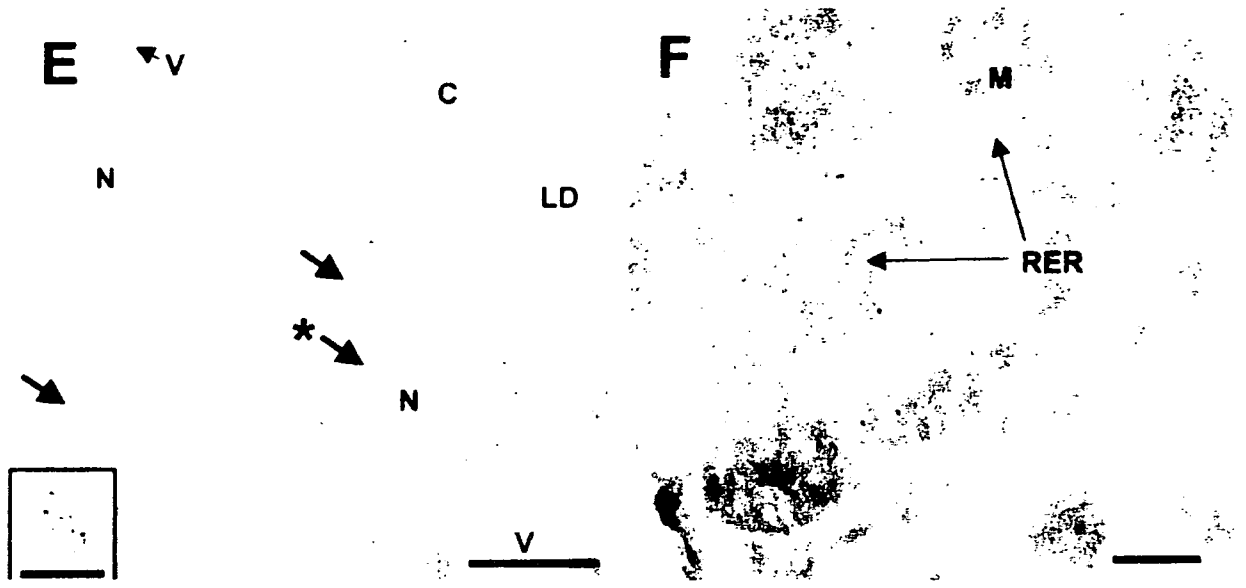

FIG. 3—*Continued.*

supernatant was also collected for isolation of RNA and determination of infectivity (FFU/ml). Real-time PCR suggested that maximal HCV RNA accumulation from H77 occurred at the intracellular level on day 2 and declined on day 5 (Fig. 4C). We observed a higher genome copy number and infectious virus titer on day 4. Similarly, JFH1 RNA-transfected IHH supernatant displayed a peak genome copy number per ml of 10^8 and infectivity of $\sim 7 \times 10^4$ FFU/ml on day 4.

HCV-infected patient serum (OP1843) displaying neutralizing activity against the vesicular stomatitis virus/HCV pseudotype (19) was used in determining neutralization of cell culture-grown HCV. Serum from a healthy volunteer was used as a negative control in HCV neutralization assays. A twofold serial dilution of heat-inactivated serum was incubated with ~100 FFU of HCV generated from the H77 clone at 37°C for 30 min. The virus-serum mixture was added to naïve IHH and incubated for 3 days. Neutralization was determined by measuring inhibition of NS5a protein expression by immunofluorescence. The results are shown as the percent inhibition based on focus-forming units per milliliter (Fig. 4D). Infectivity (~60%) was inhibited by prior incubation of HCV in culture medium with the patient serum at a 1/50 dilution. Inhibition was also observed at different dilutions of sera from three other HCV-infected patients. In contrast, sera from four healthy individuals did not inhibit infectivity at a 1/10 dilution. These results suggest that infectious HCV particles released in the culture medium are neutralized by specific antibodies.

HCV RNA is directly translated, and the precursor viral polypeptide is cleaved proteolytically to form individual proteins. The replicase complex amplifies the RNA via a minus-strand intermediate. Plus-strand RNA progeny are packaged into virus particles and acquire their envelopes probably by budding into the lumen of the endoplasmic reticulum. HCV particles are likely to be exported via the constitutive secretory pathway. Based on this working principle, we have shown in this report that IHH support HCV genome replication and protein expression from genotype 1a. Immunogold labeling using a monoclonal antibody demonstrated localization of HCV E1 glycoprotein in the rough endoplasmic reticulum and the formation of virus-like particles. We transferred culture media of HCV-replicating cells into naïve IHH, and HCV infection was detected by RT-PCR and indirect immunofluorescence. We have also observed JFH1 replication and virus growth in IHH. The infectious units appeared to be similar for JFH1 grown in Huh-7 cells and in its derivatives. JFH1 may replicate with a higher efficiency than H77 at the RNA level in Huh-7 cells or its derivatives. However, we focused on determining the generation of infectious HCV from H77 and JFH1 in IHH. In our experimental system, we observed that virus genome copies of H77 and JFH1 were at similar levels in H77 and JFH1 RNA-transfected culture supernatant. The number of focus-forming units per milliliter of H77 and JFH1 was also similar. We did not purify virus particles for negative staining due to the relatively low number of infectious units in the culture media. Three different groups of investigators have reported different densities of HCV genotype 2a particles. Zhong et al. (33) observed peak infectivity at an apparent density of 1.105 gm/ml, and Wakita et al. (29) observed peak infectivity at a density of ~1.15 gm/ml. Lidenbach et al. (15) observed a broad distribution of virus infectivity over a range of 1.01 to 1.12 gm/ml. A similar finding suggesting variation of between 1.06 and 1.16 gm/ml in buoyant density of cell culture-grown HCV genotype 2a was reported by Cai et al. (5). HCV is known to associate with serum immunoglobulin and lipoproteins (24). We have observed HCV infectivity within a density range of 1.09 to 1.12 in sucrose gradients, which did not correlate with highest copy number of virus genomic RNA (data not shown).

Recently, HCV production from a HCV-ribozyme construct of genotype 1a (clone H77) in Huh-7 cells was reported, although the infectivity of the virus was not determined (8). Virus genome replication and assembly are multistep processes and are influenced by the intracellular milieu. Inhibition of host cell growth

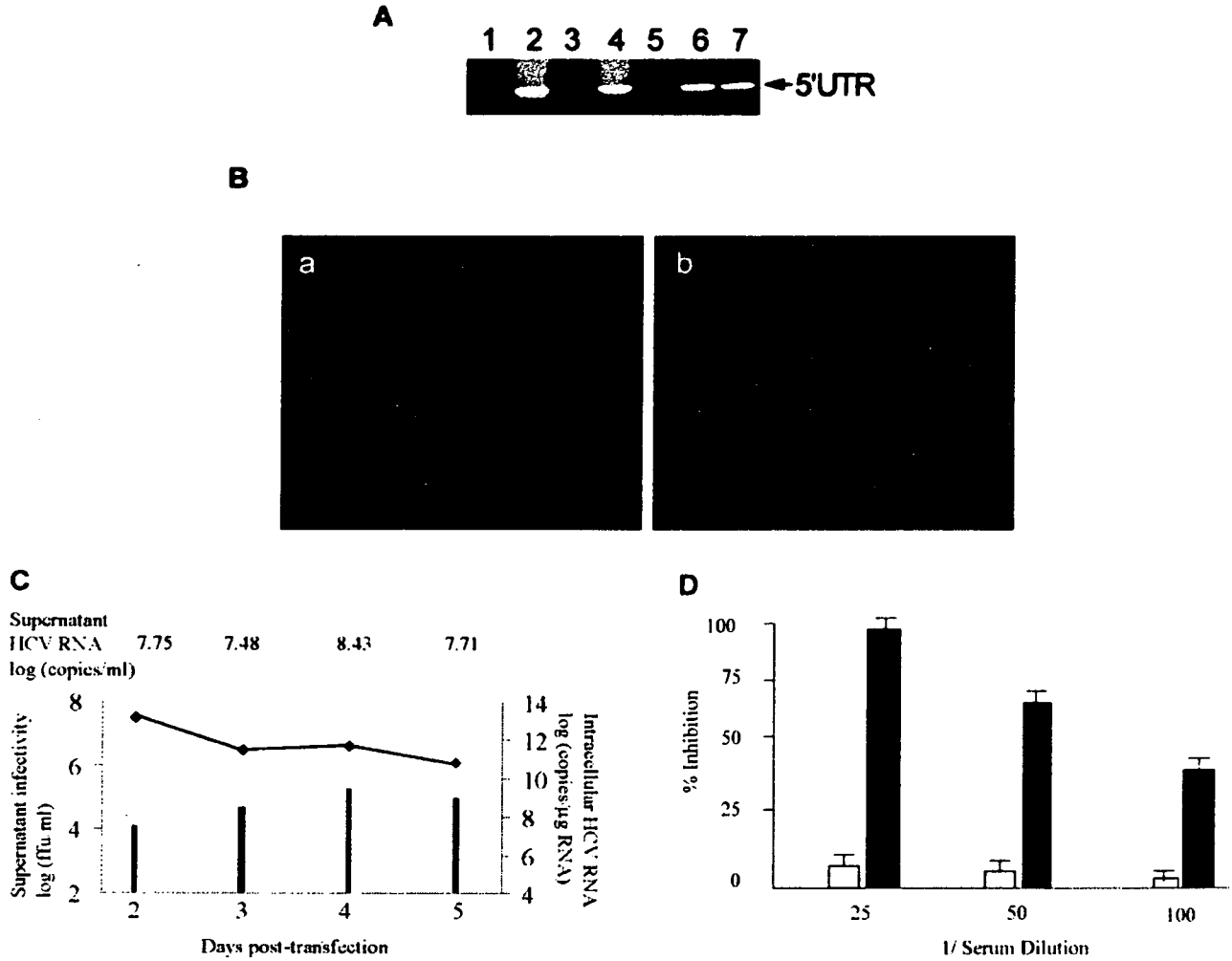

FIG. 4. Presence of HCV in culture medium and infectivity of naïve IHH. (A) RT-PCR analysis was performed using sequence-specific primers for detection of 5'UTR from culture medium of HCV RNA-transfected IHH. Filtered culture medium from IHH transfected with H77/GND RNA (lane 1), full-length H77 RNA (lane 2), JFH1/GND (lane 3), or full-length JFH1 RNA (lane 4) was analyzed for amplification of 5'UTR. The HCV genome was amplified similarly from Huh-7 cells transfected with JFH1/GND RNA (lane 5) or full-length JFH1 RNA (lane 6). Cloned H77 DNA was included as a positive control in PCR amplification (lane 7). (B) Immunofluorescence of IHH at day 3 after infection with filtered culture medium from H77 (a) or JFH1 (b) for detection of NS5a or NS3 protein expression, respectively. (C) Generation of infectious HCV after transfection of H77 genomic RNA into IHH. In vitro-transcribed H77 RNA (2 μg) was introduced into 1×10^6 IHH by electroporation. Copies of HCV RNA at the intracellular (◆) level and in the culture supernatant (numbers on top) were measured by real-time PCR on the indicated days. Infectivity of the virus in the supernatant of cultures of naïve IHH was determined and is expressed as FFU/ml (black bars). (D) Neutralization of virus infectivity by HCV-infected patient serum (black bars). Twofold serial dilutions of test serum were incubated with ~100 focus-forming units of virus generated from the H77 clone at 37°C for 30 min. The virus-serum mixture was added to naïve IHH and incubated for 3 days for determination of focus-forming units of NS5a protein by indirect immunofluorescence, using NS5a-specific antibody. A similar experiment was performed in parallel with serum from a healthy individual (hatched bars). The results are presented as the percent inhibition of virus infectivity measured in focus-forming units, and variations from triplicate assays are indicated by error bars.

and induction of cytokines, such as interferons, may have an impact on virus replication (3). Our study supports proof of the concept of HCV replication and assembly of genotype 1a in IHH. To our knowledge, this is the first report describing the generation of cell culture-grown HCV from genotype 1a. We speculate that cellular defense mechanisms against HCV infection are attenuated or compromised in IHH. Further studies may help to unravel the specific mechanisms for growth of HCV in IHH and to address important biological questions about the life cycle of HCV. Studies are in progress to determine the factors influencing virus growth, such as serial passage for adaptation in IHH, mutations at specific sites on the HCV genome, and selection of cell populations for attenuated protective mechanisms. We will also characterize the biophysical properties of cell culture-grown HCV and its infectivity in available animal models in the near future.

We are grateful to Charles M. Rice for providing the full-length H77 clone, Michael Houghton for the E1 monoclonal antibody, Arvind Patel for antiserum to core protein, George Luo for monoclonal antibody to NS3 protein, and Leonard E. Grosso for detection of HCV

RNA. We appreciate the helpful suggestions of Richard W. Compans concerning electron microscopy and Francis V. Chisari in determining virus infectivity. We thank Lin Cowick for preparation of the manuscript.

This work was supported by research grants AI45144 (R.B.R.) and CA85486 (R.R.) from the National Institutes of Health. T.W. was partly supported by grants from the Ministry of Health, Labor and Welfare of Japan, the Program for Promotion of Fundamental Studies in Health Sciences of the National Institute of Biomedical Innovation (NIBIO), and Research on Health Sciences focusing on Drug Innovation from the Japan Health Sciences Foundation.

ADDENDUM

While our manuscript was under revision, Yi et al. (31) reported the growth of H77-S in Huh-7.5 cells.

REFERENCES

1. **Basu, A., K. Meyer, R. B. Ray, and R. Ray.** 2001. Hepatitis C virus core protein modulates the interferon-induced transacting factors of JAK/Stat signaling pathway but does not affect the activation of IRF-1 or 561 genes. Virology **288**:379–390.
2. **Basu, A., K. Meyer, R. B. Ray, and R. Ray.** 2002. Hepatitis C virus core protein is necessary for the maintenance of immortalized human hepatocytes. Virology **298**:53–62.
3. **Blight, K. J., J. A. McKeating, J. Marcotrigiano, and C. M. Rice.** 2003. Efficient replication of hepatitis C virus genotype 1a RNAs in cell culture. J. Virol. **77**:3181–3190.
4. **Bode, J. G., S. Ludwig, C. Ehrhardt, U. Albrecht, A. Erhardt, F. Schaper, P. C. Heinrich, and D. Haussinger.** 2003. IFN-α antagonistic activity of HCV core protein involves induction of suppressor of cytokine signaling-3. FASEB J. **17**:488–490.
5. **Cai, Z., C. Zhang, K. S. Chang, J. Jiang, B. C. Ahn, T. Wakita, T. J. Liang, and G. Lou.** 2005. Robust production of infectious hepatitis C virus (HCV) from stably HCV cDNA-transfected human hepatoma cells. J. Virol. **79**: 13963–13973.
6. **Di Bisceglie, A. M., R. L. Carithers, and G. J. Gores.** 1998. Hepatocellular carcinoma. Hepatology **28**:1161–1165.
7. **Hayashi, J., H. Aoki, Y. Arakawa, and O. Hino.** 1999. Hepatitis C virus and hepatocarcinogenesis. Intervirology **42**:205–210.
8. **Heller, T., S. Saito, J. Auerbach, T. Williams, T. R. Moreen, A. Jazwinski, B. Cruz, N. Jeurkar, R. Sapp, G. Luo, and T. J. Liang.** 2005. An in vitro model of hepatitis C virion production. Proc. Natl. Acad. Sci. USA **102**:2579–2583.
9. **Hoofnagle, J. H., and A. M. Di Bisceglie.** 1997. The treatment of chronic viral hepatitis. N. Engl. J. Med. **336**:347–356.
10. **Ikeda, M., M. Yi, K. Li, and S. M. Lemon.** 2002. Selectable subgenomic and genome-length dicistronic RNAs derived from an infectious molecular clone of the HCV-N strain of hepatitis C virus replicate efficiently in cultured Huh7 cells. J. Virol. **76**:2997–3006.
11. **Jeffers, L.** 2000. Hepatocellular carcinoma: an emerging problem with hepatitis C. J. Natl. Med. Assoc. **92**:369–371.
12. **Kato, T., A. Furusaka, M. Miyamoto, T. Date, K. Yasui, J. Hiramoto, K. Nagayama, T. Tanaka, and T. Wakita.** 2001. Sequence analysis of hepatitis C virus isolated from a fulminant hepatitis patient. J. Med. Virol. **64**:334–339.
13. **Kolykhalov, A. A., E. V. Agapov, K. J. Blight, K. Mihalik, S. M. Feinstone, and C. M. Rice.** 1997. Transmission of hepatitis C by intrahepatic inoculation with transcribed RNA. Science **277**:570–574.
14. **Kolykhalov, A. A., K. Mihalik, S. M. Feinstone, and C. M. Rice.** 2000. Hepatitis C virus-encoded enzymatic activities and conserved RNA elements in the 3′ nontranslated region are essential for virus replication in vivo. J. Virol. **74**:2046–2051.
15. **Lindenbach, B. D., M. J. Evans, A. J. Syder, B. Wolk, T. L. Tellinghuisen, C. C. Liu, T. Maruyama, R. O. Hynes, D. R. Burton, J. A. McKeating, and C. M. Rice.** 2005. Complete replication of hepatitis C virus in cell culture. Science **309**:623–626.
16. **Lin, W., W. H. Choe, Y. Hiasa, Y. Kamegaya, J. T. Blackard, E. V. Schmidt, and R. T. Chung.** 2005. Hepatitis C virus expression suppresses interferon signaling by degrading STAT1. Gastroenterology **128**:1034–1041.
17. **Majumder, M., A. K. Ghosh, R. Steele, X. Y. Zhou, N. J. Phillips, R. Ray, and R. B. Ray.** 2002. Hepatitis C virus NS5A protein impairs TNF-mediated hepatic apoptosis, but not by an anti-FAS antibody, in transgenic mice. Virology **294**:94–105.
18. **Melen, K., R. Fagerlund, M. Nyqvist, P. Keskinen, and I. Julkunen.** 2004. Expression of hepatitis C virus core protein inhibits interferon-induced nuclear import of STATs. J. Med. Virol. **73**:536–547.
19. **Meyer, K., A. Beyene, T. L. Bowlin, A. Basu, and R. Ray.** 2004. Coexpression of hepatitis C virus E1 and E2 chimeric envelope glycoproteins displays separable ligand sensitivity and increases pseudotype infectious titer. J. Virol. **78**:12838–12847.
20. **Miller, K., S. McArdle, M. J. Gale, Jr., D. A. Geller, B. Tenoever, J. Hiscott, D. R. Gretch, and S. J. Polyak.** 2004. Effects of the hepatitis C virus core protein on innate cellular defense pathways. J. Interferon Cytokine Res. **24**:391–402.
21. **Moradpour, D., and H. E. Blum.** 1999. Current and evolving therapies for hepatitis C. Eur. J. Gastroenterol. Hepatol. **11**:1199–1202.
22. **Pawlotsky, J. M.** 2005. Current and future concepts in hepatitis C therapy. Semin. Liver Dis. **25**:72–83.
23. **Pietschmann, T., V. Lohmann, A. Kaul, N. Krieger, G. Rinck, G. Rutter, D. Strand, and R. Bartenschlager.** 2002. Persistent and transient replication of full-length hepatitis C virus genomes in cell culture. J. Virol. **76**:4008–4021.
24. **Prince, A. M., T. Huima-Byron, T. S. Parker, and D. M. Levine.** 1996. Visualization of hepatitis C virions and putative defective interfering particles isolated from low-density lipoproteins. J. Viral Hepat. **3**:11–17.
25. **Ray, R. B., K. Meyer, and R. Ray.** 2000. Hepatitis C virus core protein promotes immortalization of primary human hepatocytes. Virology **271**:197–204.
26. **Ray, R. B., and R. Ray** 2001. Hepatitis C virus core protein: intriguing properties and functional relevance. FEMS Microbiol. Lett. **202**:149–156.
27. **Saito, I., T. Miyamura, A. Ohbayashi, H. Harada, T. Katayama, S. Kikuchi, Y. Watanabe, S. Koi, M. Onji, Y. Ohta, Q. Choo, M. Houghton, and G. Kuo.** 1990. Hepatitis C virus infection is associated with the development of hepatocellular carcinoma. Proc. Natl. Acad. Sci. USA **87**:6547–6549.
28. **Simmonds, P., E. C. Holmes, T. A. Cha, S. W. Chan, F. McOmish, B. Irvine, E. Beall, P. L. Yap, J. Kolberg, and M. S. Urdea.** 1993. Classification of hepatitis C virus into six major genotypes and a series of subtypes by phylogenetic analysis of the NS-5 region. J. Gen. Virol. **74**:2391–2399.
29. **Wakita, T., T. Pietschmann, T. Kato, T. Date, M. Miyamoto, Z. Zhao, K. Murthy, A. Habermann, H. G. Krausslich, M. Mizokami, R. Bartenschlager, and T. J. Liang.** 2005. Production of infectious hepatitis C virus in tissue culture from a cloned viral genome. Nature Med. **11**:791–796.
30. **Yanagi, M., R. H. Purcell, S. U. Emerson, and J. Bukh.** 1997. Transcripts from a single full-length cDNA clone of hepatitis C virus are infectious when directly transfected into the liver of a chimpanzee. Proc. Natl. Acad. Sci. USA **94**:8738–8743.
31. **Yi, M., R. A. Villanueva, D. L. Thomas, T. Wakita, and S. M. Lemon.** 6 February 2006, posting date. Production of infectious genotype 1a hepatitis C virus (Hutchinson strain) in cultured human hepatoma cells. Proc. Natl. Acad. Sci. USA **103**:2310–2315. [Online.]
32. **Zein, N. N., J. Rakela, E. L. Krawitt, K. R. Reddy, T. Tominaga, and D. H. Persing.** 1996. Hepatitis C virus genotypes in the United States: epidemiology, pathogenicity, and response to interferon therapy. Ann. Intern. Med. **124**:634–639.
33. **Zhong, J., P. Gastaminza, G. Cheng, S. Kapadia, T. Kato, D. R. Burton, S. F. Wieland, S. L. Uprichard, T. Wakita, and F. V. Chisari.** 2005. Robust hepatitis C virus infection in vitro. Proc. Natl. Acad. Sci. USA **102**:9294–9299.

JOURNAL OF VIROLOGY, May 2006, p. 4510–4520 Vol. 80, No. 9
0022-538X/06/$08.00+0 doi:10.1128/JVI.80.9.4510–4520.2006

Diverse Effects of Cyclosporine on Hepatitis C Virus Strain Replication

Naoto Ishii,[1]† Koichi Watashi,[1]† Takayuki Hishiki,[1] Kaku Goto,[1] Daisuke Inoue,[1] Makoto Hijikata,[1] Takaji Wakita,[2] Nobuyuki Kato,[3] and Kunitada Shimotohno[1]*

Laboratory of Human Tumor Viruses, Department of Viral Oncology, Institute for Virus Research, Kyoto University, Kyoto,[1] Department of Microbiology, Tokyo Metropolitan Institute for Neuroscience, Tokyo,[2] and Department of Molecular Biology, Okayama University Graduate School of Medicine, Dentistry and Pharmaceutical Sciences, Okayama,[3] Japan

Received 18 December 2005/Accepted 10 February 2006

Recently, a production system for infectious particles of hepatitis C virus (HCV) utilizing the genotype 2a JFH1 strain has been developed. This strain has a high capacity for replication in the cells. Cyclosporine (CsA) has a suppressive effect on HCV replication. In this report, we characterize the anti-HCV effect of CsA. We observe that the presence of viral structural proteins does not influence the anti-HCV activity of CsA. Among HCV strains, the replication of genotype 1b replicons was strongly suppressed by treatment with CsA. In contrast, JFH1 replication was less sensitive to CsA and its analog, NIM811. Replication of JFH1 did not require the cellular replication cofactor, cyclophilin B (CyPB). CyPB stimulated the RNA binding activity of NS5B in the genotype 1b replicon but not the genotype 2a JFH1 strain. These findings provide an insight into the mechanisms of diversity governing virus-cell interactions and in the sensitivity of these strains to antiviral agents.

Hepatitis C virus (HCV), a member of the *Flaviviridae* family, has a positive-strand RNA genome (1, 26). The genome encodes a large precursor polyprotein, which is cleaved by host and viral proteases to generate at least 10 functional viral proteins: core, envelope 1 (E1), E2, p7, nonstructural protein 2 (NS2), NS3, NS4A, NS4B, NS5A, and NS5B (6, 8). NS5B is an RNA-dependent RNA polymerase that is crucial for viral genome replication (1, 26). There is genetic heterogeneity within the HCV genome. Currently, these differences are classified into six genotypes that are further segregated into a series of subtypes (4, 23). In Japan, genotype 1b is predominant; roughly 65% of cases of HCV-related chronic hepatitis involve genotype 1b. By comparison, genotype 2a is present in 17% of these patients (13, 23).

Sustained infection of HCV is the major cause of chronic liver diseases such as chronic hepatitis, liver cirrhosis, and hepatocellular carcinoma (16). Rarely, HCV causes fulminant hepatitis (13). The predominant treatment for HCV-infected patients is interferon (IFN) or polyethylene glycol-conjugated IFN alone or in combination with ribavirin (19, 20). However, alternative anti-HCV therapies are needed because virus is not eliminated in about half of the treated patients (19, 20). Lohmann et al. have developed the HCV subgenomic replicon system, in which an HCV subgenomic replicon autonomously replicates in Huh-7 cells (HCV replicon cells) (18). This replicon comprises the HCV 5′ untranslated region (5′UTR) containing an internal ribosomal entry site (IRES), the neomycin phosphotransferase gene, the encephalomyocarditis virus (EMCV) IRES, the coding region for HCV NS3 through NS5B, and the HCV 3′UTR (subgenomic replicon), but it lacks the coding region for the core and envelope proteins, as well as p7 and NS2 (Fig. 1). Subsequently, a genome-length (full-genome) replicon has been developed. This construct contains a full-genome length of HCV, including the coding regions for the core protein through NS2 (Fig. 1) (5, 10). We can evaluate HCV replication using these subgenomic or genome-length replicon systems. Previously, we established HCV subgenomic replicon cells carrying HCV genotype 1b NN strain (15, 29). We demonstrated that an immunosuppressant, cyclosporine (CsA), has anti-HCV activity in these cells (29). In addition, we determined the molecular mechanism of the anti-HCV effect of CsA on this replicon; cyclophilin B (CyPB), one of the cellular targets of CsA, is a cellular replication cofactor of the HCV genome (31). CyPB interacts with NS5B to promote its RNA binding activity (for a detailed description, see reference 31). CsA is suggested to suppress HCV genome replication by inhibiting the functional association of CyPB with NS5B. Another group also reported anti-HCV function of CsA using a subgenomic replicon of other genotype 1b strain, HCV-N (22). In this study, we demonstrate that CsA also has a strong anti-HCV activity in other available genotype 1b replicons carrying the Con1 and O strains (12, 18).

Recently, Wakita and colleagues reported that a replicon of HCV genotype 2a JFH-1 strain, which was isolated from a case of type-C fulminant hepatitis, has a much stronger level of replication activity than genotype 1b replicons in Huh-7 cells (13, 27). A production system of infectious viral particles was recently established with this high-replication-competent strain (17, 27, 34). This viral strain may acquire a growth advantage compared with many other strains, although the underlying mechanism is unknown. In this study, we described a characteristic difference in the replication of JFH1 compared to that of genotype 1b replicons.

Here, we report that JFH1 replication is less sensitive to CsA than genotype 1b strains, although the interaction of

* Corresponding author. Mailing address: Laboratory of Human Tumor Viruses, Department of Viral Oncology, Institute for Virus Research, Kyoto University, 53 Kawaharacho, Shogoin, Sakyo-ku, Kyoto 606-8507, Japan. Phone: 81-75-751-4000. Fax: 81-75-751-3998. E-mail: kshimoto@virus.kyoto-u.ac.jp.
† N.I. and K.W. contributed equally to this work.

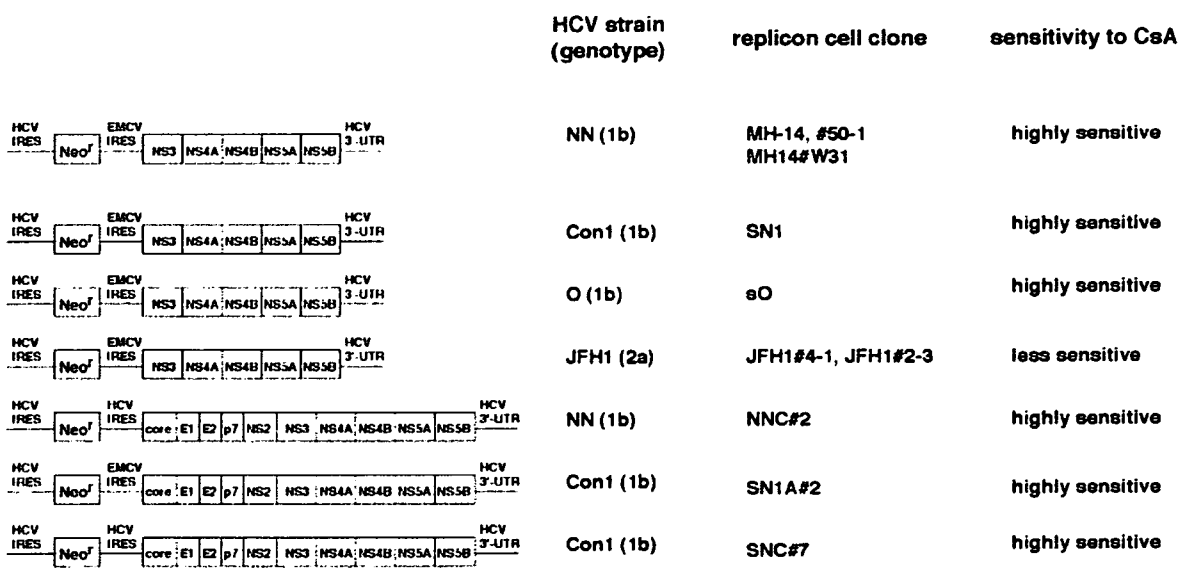

FIG. 1. Schematic representation of the constructs of HCV subgenomic and genome-length replicon RNA. On the left, the constructs of each replicon RNA are shown. HCV strains, as well as genotypes from which the replicon RNA sequences are derived, are indicated in the second column. The names of replicon cell clones established with each replicon RNA are in the third column. The sensitivity to CsA of each replicon RNA revealed in this study is summarized in the fourth column. The replicon RNAs comprise the HCV 5'UTR, including HCV IRES, the neomycin phosphotransferase gene (Neo^r), EMCV IRES, or HCV IRES, the coding region for HCV proteins NS3 to NS5B (subgenomic) or core to NS5B (genome length or full genome), and HCV 3'UTR. MH-14 (NN/1b/SG), #50-1 (NN/1b/SG), MH14#W31 (NN/1b/SG), SN1 (Con1/1b/SG), sO (O/1b/SG), JFH1#4-1 (JFH1/2a/SG), and JFH1#2-3 (JFH1/2a/SG) cells carry subgenomic replicons, while NNC#2 (NN/1b/FL), SN1A#2 (Con1/1b/FL), and SNC#7 (Con1/1b/FL) cells have genome-length replicons. NNC#2 (NN/1b/FL) and SNC#7 (Con1/1b/FL) cells contain the replicon RNA without EMCV IRES.

CyPB with NS5B is observed with this replicon. However, genome replication and RNA binding activity of NS5B are independent of CyPB. We have exploited a chemical compound to demonstrate how strain diversity can be generated by underlying differences in the mechanisms of the virus-cell interaction. These findings provide important insight into the mechanisms that mediate the efficacy of antiviral agents.

MATERIALS AND METHODS

Cell culture. Huh-7 cells were cultured in Dulbecco's modified Eagle medium (Invitrogen) with 10% fetal bovine serum, nonessential amino acids (Invitrogen), and L-glutamine (Invitrogen). MH-14, #50-1, MH14#W31, SN1, sO (formerly named 1B2R1), JFH1#4-1, and JFH1#2-3 cells (12, 13, 15, 18, 29), carrying subgenomic replicons, and NNC#2, SN1A#2, and SNC#7 cells, carrying full-genome replicons, were cultured in the above medium supplemented with 300- to 500-μg/ml G418 (Invitrogen). In the assay measuring the response to CsA, NIM811, or PSC833 (Fig. 2, 3, and 4), we seeded small numbers of each replicon cells (7×10^3 to 15×10^3 cells/12-well plate) and treated with each drug. Culture medium was changed every 3 days (CsA, NIM811, or PSC833 was supplemented in the fresh medium for the treatment groups). We did not perform any passages in the assay period. At day 7, the cells were 70 to 90% confluent. A schematic representation of the constructs of HCV replicon RNAs, the name of HCV strains from which the replicon RNA sequences are derived, and the name of replicon cell clones used in this study are summarized in Fig. 1. Since many replicon clones were used in this study, we list "strain/genotype/length of the replicon construct" in parentheses after the names of each cell clone in Results and in the figure legends to avoid confusion between names: for example, MH-14 (NN/1b/SG), JFH1#4-1 (JFH1/2a/SG), and SN1A#2 (Con1/1b/FL) cells. The designations SG and FL indicate subgenomic and full-genome replicons, respectively.

Establishment of replicon cells. MH-14, #50-1, sO, JFH1#4-1, and JFH1#2-3 cells were described previously (12, 13, 15, 29). The replicon RNAs were produced using a MEGAscript T7 kit (Ambion) from pMH14, pSN1, pNNC, pSN1A, and pSNC plasmids for the establishment of the MH14#W31, SN1, NNC#2, SN1A#2, and SNC#7 replicon cells, respectively. For the establishment of MH14#W31, we transfected RNA into the Huh-7 cell strain which was identical to the parental cells of JFH1#4-1 and JFH1#2-3. Each replicon RNA was transfected into Huh-7 cells, following the selection with the medium in the presence of 500- to 1,000-μg/ml G418 for around 4 weeks. The resultant cell colonies were isolated and expanded. The HCV RNA titers in cell clones carrying JFH1 replicons were not significantly different from those in established cell clones carrying genotype 1b replicons.

Plasmid construction. pSN1, the sequence of which is derived from I377NS3-3' (18), was prepared essentially as described previously (15). pSN1A was generated by inserting the region from the core to NS2 of pM1LE (15) into the upstream coding region for NS3 in pSN1. To obtain pSNC, the EMCV IRES of pSN1A was replaced by the HCV IRES. pNNC was produced by inserting the coding region from NS3 to NS5B of pM1LE into pSNC.

Real-time reverse transcription-PCR (RT-PCR) analysis. The 5'UTR of HCV genome RNA was quantified using the ABI PRISM 7700 sequence detector (Applied Biosystems) as described previously (29).

Immunoblot analysis. Immunoblot analysis was performed as described previously (30). The primary antibodies used in this study were anti-core, anti-E2 (kindly provided by M. Kohara, Tokyo Metropolitan Institute of Medical Science), anti-NS3, anti-NS5A (a generous gift from A. Takamizawa, Osaka University), anti-NS5B (NS5B-6; kindly provided by I. Fukuya, Osaka University), anti-CyPA (Upstate Cell Signaling), anti-CyPB (Affinity BioReagents), and anti-tubulin (Oncogene).

Immunoprecipitation assay and RNA-protein binding precipitation assay. Immunoprecipitation and RNA-protein binding precipitation were performed as described previously (30, 31).

RNA interference technique. The condition of small interfering RNA (siRNA) used in this study was described previously (31). Transfection was performed using siLentFect (Bio-Rad), according to the manufacturer's protocol.

Isolation of replication complex. The HCV replication complex was isolated from cells by treatment with 50-μg/ml digitonin at 27°C for 5 min, following treatment with 0.3-μg/ml proteinase K at 37°C for 5 min as described previously (31).

Purification of recombinant GST-fused CyPB protein. Glutathione *S*-transferase (GST) and GST-fused CyPB (GST-CyPB) protein expression was induced

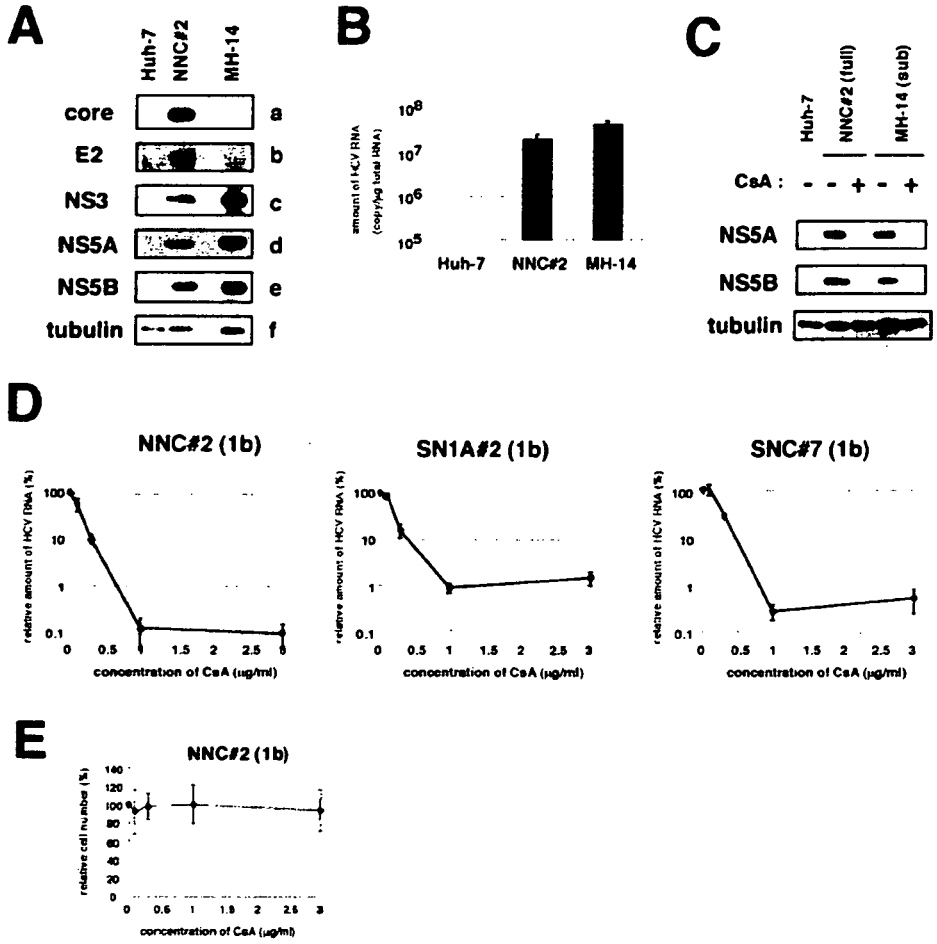

FIG. 2. CsA suppressed the replication of HCV genome, irrespective of the presence of the structural proteins. (A) Detection of HCV proteins from NNC#2 (NN/1b/FL) genome-length replicon. Core (a), E2 (b), NS3 (c), NS5A (d), NS5B (e), and tubulin (f) in Huh-7, NNC#2 (NN/1b/FL), and MH-14 (NN/1b/SG) cells analyzed by immunoblot analysis are shown. (B) HCV RNA in Huh-7, NNC#2 (NN/1b/FL), and MH-14 (NN/1b/SG) cells quantified by real-time RT-PCR analysis. The data represent the means of three independent experiments. (C) CsA decreased the production of HCV proteins in NNC#2 (NN/1b/FL), as well as in MH-14 (NN/1b/SG) cells. After treatment with 1-μg/ml CsA (+) for 5 days or without treatment (−), total-cell lysates of NNC#2 (NN/1b/FL) and MH-14 (NN/1b/SG) cells, together with Huh-7 cells as a negative control, were recovered to examine the production of HCV NS5A (top), NS5B (middle), and tubulin as an internal control (bottom) by immunoblot analysis. The same result was obtained at day 7 after treatment. (D) The sensitivity to CsA of HCV genome-length replicon was almost the same as that of the subgenomic replicon. HCV RNA was quantified by real-time RT-PCR analysis using total RNA from NNC#2 (NN/1b/FL), SN1A#2 (Con1/1b/FL), and SNC#7 (Con1/1b/FL) cells treated with various concentrations of CsA for 7 days. The relative amount of HCV RNA was plotted against the concentration of CsA (in micrograms per milliliter). (E) Effect of CsA on cell proliferation. NNC#2 (NN/1b/FL) cells were treated with various amount of CsA for 7 days. Cell numbers were counted, and cell numbers relative to those of cells without treatment were plotted against the concentration of CsA.

in transformed BL21 cells (Amersham) with 1 mM isopropyl-β-thiogalactopyranoside (IPTG). The cell lysate was incubated with glutathione-Sepharose resin (Amersham) and washed extensively. The recombinant protein was eluted by glutathione (pH 8.0) and subsequently dialyzed.

In vitro RNA binding assay. In vitro-translated ^{35}S-labeled NS5B proteins and poly(U)-Sepharose (Amersham) or protein G-Sepharose (Amersham) resin as a negative control were incubated in the presence of recombinant GST-CyPB protein at 4°C for 1 h. After being washed, precipitates were fractionated by sodium dodecyl sulfate-polyacrylamide gel electrophoresis and analyzed by imaging analyzer.

RESULTS

CsA suppressed the replication of HCV full-genome replicon. We and another group have reported an anti-HCV activity of CsA using subgenomic replicons (22, 29). HCV structural proteins, especially the core protein, have multiple functions. These proteins interact with many cellular factors and modulate a variety of cellular functions (32). Potentially, these viral proteins could diminish or circumvent the suppression of HCV genome replication by CsA. Core protein and E2 reportedly modulate the activity of IFN signaling (9, 25). To test this possibility, we established a full-genome HCV replicon system with cells transfected with the NN strain (NNC#2 cells [NN/1b/FL]) (Fig. 1). HCV RNA and protein productions were confirmed by real-time RT-PCR and immunoblot analysis (Fig. 2A and B). In addition, we confirmed that this replication was not due to the integration of the replicon construct into the

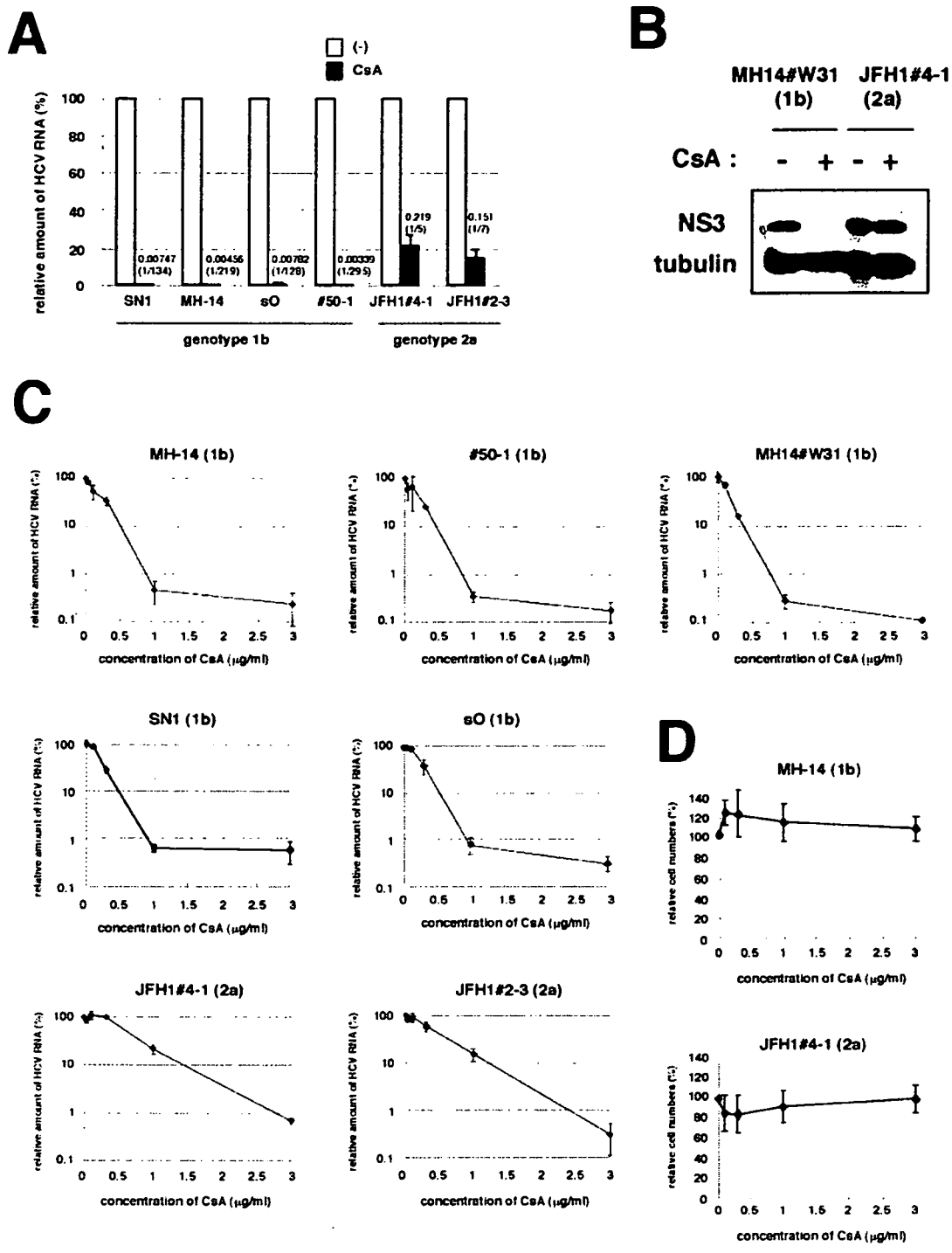

FIG. 3. Replication of a genotype 2a strain, JFH1, was less sensitive to CsA. (A) Sensitivity to CsA of HCV genotype 1b and JFH1 replicons. SN1 (Con1/1b/SG), MH-14 (NN/1b/SG), sO (O/1b/SG), #50-1 (NN/1b/SG), JFH1#4-1 (JFH1/2a/SG), and JFH1#2-3 (JFH1/2a/SG) cells, carrying HCV subgenomic replicon, were treated with 1-μg/ml CsA for 7 days. HCV RNA titers were quantified by real-time RT-PCR analysis, and the relative amounts are shown. The bars represent the means of three independent experiments. White bars, no treatment; black bars, 1-μg/ml CsA. The numbers above the black bars indicate fold difference of the titer with 1-μg/ml CsA treatment compared to no treatment. (B) Levels of NS3 and tubulin as an internal control in MH14#W31 (NN/1b/SG) and JFH1#4-1 (JFH1/2a/SG) cells without (−) or with (+) 1-μg/ml CsA treatment for 5 days were detected by immunoblot analysis. (C) HCV RNA was quantified and plotted as described in the legend to Fig. 2D with genotype 1b replicon cells such as MH-14 (NN/1b/SG), #50-1 (NN/1b/SG), MH14#W31 (NN/1b/SG), SN1 (Con1/1b/SG), and sO (O/1b/SG) cells and JFH1-carrying replicon cells such as JFH1#4-1 (JFH1/2a/SG) and JFH1#2-3 (JFH1/2a/SG) cells. (D) Effect of CsA on cell proliferation. The growth of MH-14 (NN/1b/SG) and JFH1#4-1 (JFH1/2a/SG) cells were examined as described in the legend for Fig. 2E.